Radiative Proton Capture by Ni^{58}, Ni^{60}, and Co^{59}

J. W. Butler and C. R. Gossett
Nucleonics Division, United States Naval Research Laboratory, Washington, D. C.
(Received August 2, 1957)

Thin targets of Ni^{58}, Ni^{60}, and Co^{59} were bombarded with protons from 700 to 1900 kev. Seventeen radiative capture resonances were observed for Ni^{58}; fifty-four resonances were observed for Ni^{60}; and about 150 resonances were observed for Co^{59}. Precise bombarding energies were determined for the nickel resonances, and are listed in tabular form. All resonances were narrower than 1 kev. The $\int\sigma(E)dE$ was measured for each of the nickel resonances. The following Q values were determined: $Ni^{58}(p,\gamma)Cu^{59}$, 3.42±0.02 Mev; $Ni^{60}(p,\gamma)Cu^{61}$, 4.81±0.03 Mev. The following low-energy cascade gamma rays were observed: Ni^{58}, 0.492±0.005, 0.908±0.020, 1.38±0.03, 1.78±0.02, 2.00 ±0.04, and 2.32±0.04 Mev; Ni^{60}, 0.468±0.010, 0.96±0.02, 1.30±0.02, 1.38±0.02, 1.63±0.03, and 1.91±0.03 Mev; Co^{59}, 0.47±0.02, 0.84±0.02, 0.95±0.02, 1.07±0.02, 1.17±0.02, 1.33 ±0.02, 1.64±0.03, and 1.77±0.03 Mev. Branching ratios to all states below 2 Mev were measured from several of the intense resonances in the nickel isotopes. The branching ratio measurements indicated that the low-energy member of each cascade in the nickel reactions, except possibly the 1.30-Mev gamma ray from protons on Ni^{60}, represented an excited state of the same energy; but indications for a 1.38-Mev state in Cu^{59} and a 1.63-Mev state in Cu^{61} were weak. Angular distribution measurements were made on some of the more intense resonances in the nickel isotopes, and unique spins were determined for those resonant states and for the first excited state of Cu^{59}. For the states whose spins were measured, probable parity assignments have been made. Reduced proton widths have been determined for the resonances below a bombarding energy of 1300 kev. The matrix elements for the several $E1$ and $M1$ transitions are compared with previous tabulations. Several new experimental techniques are discussed.

I. INTRODUCTION

THE existence of sharp, well-defined resonances in the yield of proton-capture gamma rays from the bombardment of nickel was discovered in this laboratory in the course of an investigation of resonances in the $O^{18}(p,\gamma)F^{19}$ reaction.[1] For that experiment, the targets were prepared by oxidizing thin (5-microinch) nickel foils with a concentrated beam of light in a partial atmosphere of enriched O^{18}. For comparison purposes, O^{16} targets were prepared in a similar manner using normal oxygen. In the resulting excitation curves, certain resonances were found which were common to both targets but were not ascribable to either oxygen isotope. They were therefore believed to be due to the nickel of the foil. To investigate this possibility, a program herein described was started using separated isotopic targets of the two most abundant isotopes of nickel: Ni^{58} (68%) and Ni^{60} (26%).

The primary motivation for beginning the experiment was the potential usefulness of the information to the low-energy experimentalist, since nickel foils are widely used as backings for thin solid targets and as windows for gas targets and gas detectors. The original plan was to determine the proton-capture excitation curve for each of the two isotopes mentioned, and to obtain some indication of the absolute cross sections and gamma-ray energies involved. However, as the work progressed, many discrepancies were found between our work and the literature (e.g., see Sec. IVB). For this reason and also because some of the preliminary results gave information of potential interest to the shell model, the scope of the experiments expanded manyfold, until in their present and final form, they include the integrated cross sections of each individual resonance observed, Q values, cascade gamma rays to low-lying states of the final nucleus, the gamma-ray branching ratios to these low-lying states for certain of the more intense resonances, angular distributions of the highest energy gamma ray from some of the resonances, the assignment of angular momentum quantum numbers and probable parity values to these states, partial and reduced proton widths, and partial and "reduced" gamma-ray widths.

The two nickel isotopes studied exhibited two fortuitous characteristics that were favorable from an experimental point of view; namely, they had abnormally low proton-capture Q values, and the spins and parities of initial and final nuclei were such as to favor ground-state gamma-ray transitions (see Sec. IVA). It was therefore decided to include in the investigation a study of the reaction, $Co^{59}(p,\gamma)Ni^{60}$, because (1) it had neither of the above-mentioned favorable characteristics, (2) it had a mass intermediate between the two nickel isotopes, and (3) the target nucleus was readily available as a naturally occurring 100% isotope.

Preliminary accounts of a part of the present work have been presented at meetings[2,3] of the American Physical Society.

II. EXCITATION CURVES

The NRL Nucleonics Division 2-Mv Van de Graaff accelerator was used as a source of protons. This accelerator will provide up to 10 or more microamperes of protons over the energy range from 300 kev to 2 Mev, with an energy spread as low as 0.03%. A 90° magnetic beam analyzer, controlled by proton magnetic-moment resonance equipment, is used to define and control the proton energy.

[1] J. W. Butler and H. D. Holmgren, Phys. Rev. **99**, 1649(A) (1955).

[2] Gossett, Butler, and Holmgren, Bull. Am. Phys. Soc. Ser. II, **1**, 40 (1956).

[3] Gossett, Butler, and Holmgren, Bull. Am. Phys. Soc. Ser. II, **1**, 223 (1956).

A. Detecting Equipment

To obtain the excitation curves, a 3-in. diam. by 3-in. long NaI(Tl) crystal was placed at 0° with respect to the beam and at a distance to subtend at the target about 40% of the total solid angle. A type 6363 multiplier phototube and conventional electronic circuits were used with a 20-channel differential pulse-height analyzer to record a profile of the pulse output of the crystal. The 20 channels were set to cover approximately the upper half of the energy spectrum of the gamma rays from the reaction under consideration. In this way, the energies of the gamma rays giving rise to each resonance were immediately apparent, and identification of gamma rays from target contaminants, such as the ubiquitous F^{19}, could usually be made.

B. Target Preparation

At first, targets were prepared by evaporation of metallic nickel onto silver disks. These proved unsatisfactory for two reasons: (1) molten nickel reacts with practically every material that would normally be used to heat it to the melting point, including carbon and iridium, and (2) a very slight amount of fluorine contamination, acquired during the evaporation process in the vacuum system, was sufficient to mask much of the gamma-ray yield from the nickel, by means of the intense well-known resonances in the $F^{19}(p,\alpha\gamma)O^{16}$ reaction.

In order to produce fluorine-free targets, the nickel was electroplated onto silver disks using a technique developed especially for the purpose. Ordinary nickel plating baths were impractical for the separated isotopes because of the amounts required. Quantitative chemical electrodeposition techniques using ammonium hydroxide were unsatisfactory also because of the amount of nickel left in solution when equilibrium was reached. Briefly, the procedure was to dissolve about 2 mg of the isotopic NiO in a concentrated solution of HCl, which was then evaporated to dryness. The residue was then redissolved in 30 ml of distilled water, and about 20 mg of boric acid added as a buffer. Deposition onto $1\frac{1}{4}$-in. diam. Ag disks was then carried out using about 20 ma of current and a platinum anode. Under these conditions, the thickness of the target, measured in kev for 1.5-Mev incident protons, was equal to the number of minutes the current flowed. The silver disks were electropolished using a cyanide bath prior to the deposition of the nickel.

C. Target Protection

Even these "clean" targets did not remain uncontaminated long once they were placed inside the Van de Graaff vacuum system and bombarded. A rather rapid buildup of fluorine was observed on a fresh nickel target during the first few minutes of bombardment. In order to obviate this second source of fluorine contamination, the target was practically surrounded with surfaces at liquid-nitrogen temperature. A cylindrical copper tube $1\frac{1}{2}$-in. diameter was placed coaxial with the beam and positioned to extend beyond the target, but not touch it, as shown in Fig. 1. This copper tube was in thermal contact with a liquid-nitrogen reservoir. At the end opposite the target were placed two diaphragms, two inches apart, each having a $\frac{1}{4}$-in. aperture to pass the proton beam. Thus the only surfaces not at liquid-nitrogen temperature which the target could "see" were those within the solid angle subtended by the $\frac{1}{4}$-in. diam aperture 12 in. from the target. The probability of an entering gas molecule striking the target without first making a cold surface collision was therefore quite small. The main body of the cold trap was not designed for the present experiments. It was used because it was immediately available, and was easily modified to the present purposes.

In addition to providing protection against fluorine contamination, this technique effectively prevented any other type of contamination, such as the formation of oil films over the target, with subsequent molecular cracking by the beam. In many reactions, such as (d,n) and (He^3,p), carbon is a source of troublesome background. Targets which had been bombarded with several microamperes of protons for several hours showed no visible traces of carbon. This technique can thus be of great usefulness in measuring resonance and threshold bombarding energies with extreme precision where thin films of pump oil or other surface contaminants would change the incident proton energy appreciably.

Using the procedures discussed above, fresh targets usually showed no evidence of fluorine. However, after prolonged bombardment, the stronger fluorine resonances would sometimes be in evidence, as will be noted later in connection with some of the excitation curves.

D. Use of Radioactivity

In cases where the residual nucleus is unstable to positron emission with a convenient half-life, the obser-

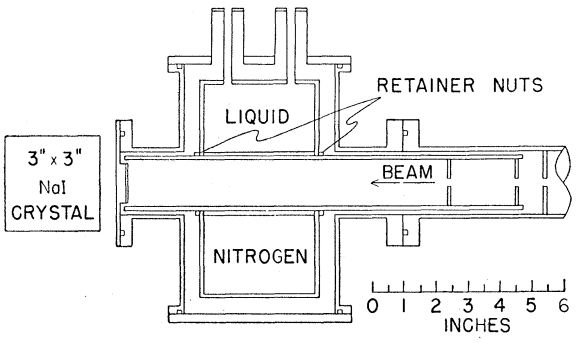

FIG. 1. Geometrical arrangement of target and crystal for excitation-curve data, showing method of protecting target from contaminants of the vacuum system. Position shown for crystal is for the crystal itself, not the sealed crystal container.

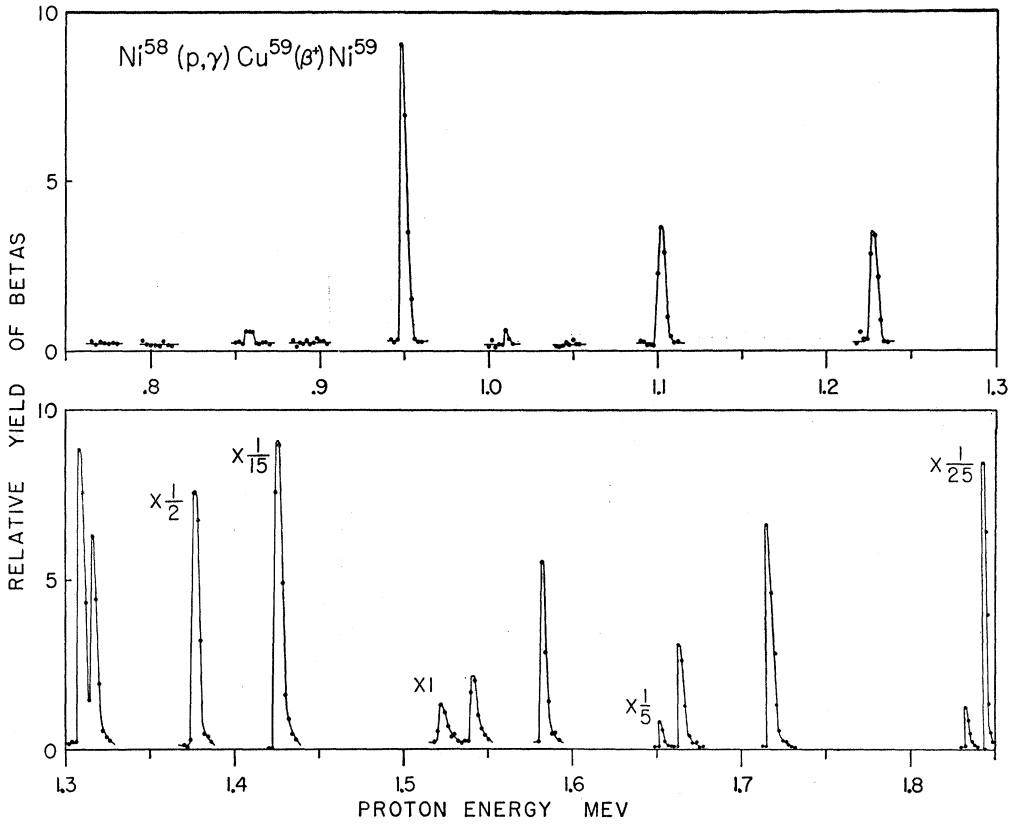

FIG. 2. Excitation function for the yield of positrons from the decay of Cu^{59} formed in the $Ni^{58}(p,\gamma)Cu^{59}$ reaction. The Ni^{58} target was about 2-kev thick to the incident protons. The blank regions in the figure showed no appreciable yield with a 15-kev target. Background counts have not been subtracted. The statistical uncertainty in the number of counts is of the order of the diameter of the solid circles.

vation of this activity provides a means of excluding the effects of fluorine or most other contamination from the excitation curves. Measurements of the half-life also aid in the interpretation of the observations because, by such measurements the target nuclide producing such radioactive product could be identified. A further advantage in the radioactivity measurements lies in the fact that all angular dependence of the yield is eliminated, so that the total integrated yield is proportional to the counting rate at any arbitrary angle.

The 81-sec half-life of Cu^{59} was quite satisfactory for this purpose, and excitation curves for the $Ni^{58}(p,\gamma)Cu^{59}$ reaction were obtained in this manner, in addition to the direct observation of the gamma rays. The 3.3-hr half-life of Cu^{61} from the $Ni^{60}(p,\gamma)Cu^{61}$ reaction was inconveniently long for this technique, and the $Co^{59}(p,\gamma)Ni^{60}$ reaction yields a stable end product.

In order to achieve a reasonably small statistical uncertainty in the positron counting rate for the $Ni^{58}(p,\gamma)Cu^{59}(\beta^+)Ni^{59}$ reaction, several bombard-count cycles at each bombarding energy were necessary in general. For this reason, an automatic cycling device was constructed to provide a 2-min bombard-count cycle. An electromagnetically driven shutter stopped the beam about 10 ft from the target.

The positrons were detected with a $1\frac{1}{2}$-in. diameter by 0.012-in. thick Pilot-B phosphor mounted on a type 6292 multiplier phototube. The experimental geometry (not shown) differed from that shown in Fig. 1 for gamma-ray detection in that the positrons were not required to pass through the brass end plate shown in Fig. 1, but instead, they passed through only the 0.010-in. Ag target backing and about $\frac{1}{16}$ in. of Al before reaching the phosphor.

E. Results

$Ni^{58}(p,\gamma)Cu^{59}$

The excitation function for the $Ni^{58}(p,\gamma)Cu^{59}(\beta^+)Ni^{59}$ reaction is shown in Fig. 2. The excitation curve was first taken in 10-kev steps with a target about 15 kev thick to 1.5-Mev incident protons (not shown). Then the curve was retaken in 2-kev steps with a 3-kev target, with data being taken at all regions showing counting rates appreciably higher than background with the thicker target. Hence the regions left blank in Fig. 2 showed no evidence of resonances with the thicker target. The data points of Fig. 2 have been corrected for the effects of residual activity from the preceding bombardment and for changes in beam intensity, but no background has been subtracted.

The gamma-ray excitation curve at 0° (not shown) showed the same resonances as the positron curve of Fig. 2, with roughly the same relative intensities. Differences in relative intensities between the two

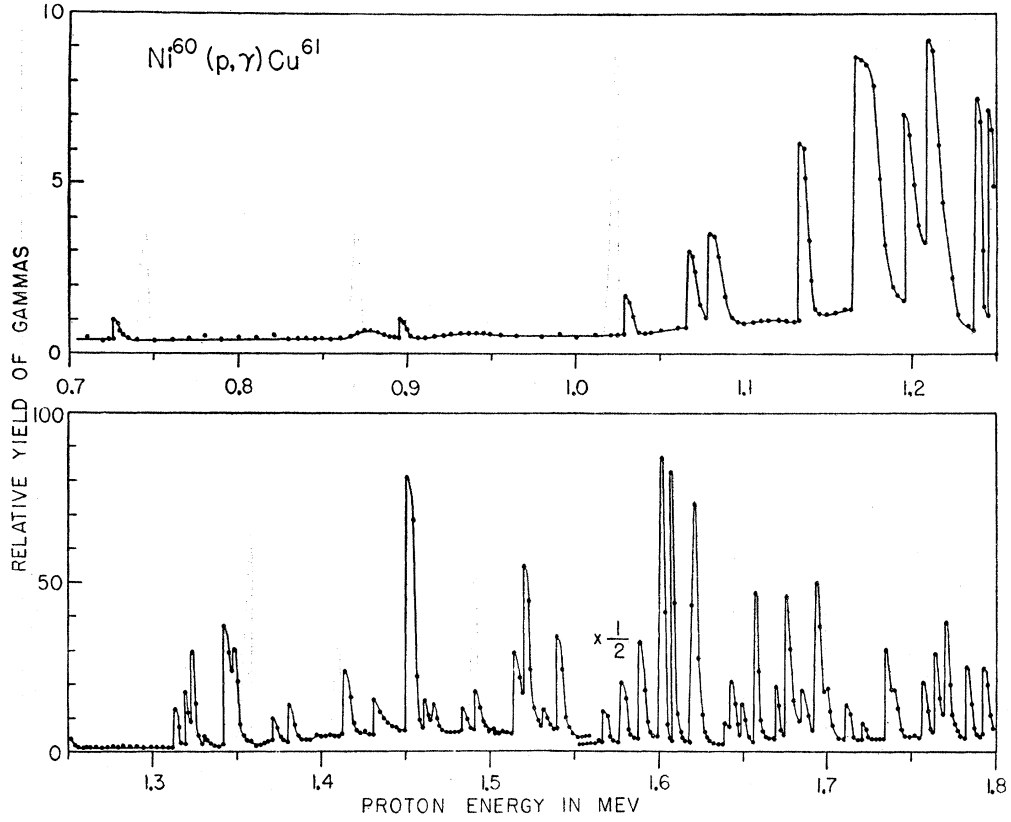

FIG. 3. Excitation function for the yield of gamma rays with energy greater than 2.7 Mev in the $Ni^{60}(p,\gamma)Cu^{61}$ reaction. Background counts have not been subtracted. The statistical uncertainty is smaller than the diameter of the solid circles.

methods of taking the data are attributed to asymmetries in the gamma-ray yield.

Seventeen resonances were found in the region studied, the lowest appearing at 855 kev. The bombarding energy at which each resonance was observed can be found by referring to Table I, discussed in Sec. III.

TABLE I. For the $Ni^{58}(p,\gamma)Cu^{59}$ reaction: resonance bombarding energies (E_p), compound-nucleus excitation energies (E_x), the "thick-target" yields (for 4π steradians) of primary gamma rays, and the integrated cross sections ($\int\sigma dE$). Uncertainties are indicated below the dimension headings. The last digit of E_x has relative significance only.

E_p (kev) (±2)	E_x (Mev) (±0.02)	Yield (γ rays/μcoul) (factor of 2)	$\int\sigma dE$ (ev barns) (factor of 2)
855	4.260	3	0.007
947	4.351	71	0.14
1010	4.413	4	0.007
1100	4.501	28	0.050
1227	4.626	26	0.045
1308	4.706	67	0.11
1316	4.714	49	0.080
1376	4.773	120	0.19
1424	4.820	1090	1.7
1522	4.916	8	0.012
1540	4.934	14	0.020
1582	4.975	46	0.066
1653	5.045	30	0.045
1663	5.055	120	0.16
1716	5.107	260	0.35
1833	5.222	50	0.063
1844	5.233	1650	2.1

The uncertainty in bombarding energies was about ±2 kev.

The proton energies at the two most intense resonances were measured very carefully by Dr. R. O. Bondelid, using a 2-meter-radius 90° electrostatic beam analyzer[4] and the large NRL Van de Graaff accelerator. His values are 1424.1±0.7 kev, and 1843.7±0.9 kev, respectively.

$Ni^{60}(p,\gamma)Cu^{61}$

The excitation curve for the $Ni^{60}(p,\gamma)Cu^{61}$ reaction is shown in Fig. 3, where the number of gamma-ray counts between 2.7 and 7 Mev is plotted against proton bombarding energy. Several different targets were used ranging in thickness from 2 kev to 7 kev. The region between 1000 kev and 1230 kev was covered with a 7-kev thick target. Some of the wider resonances conceivably could be doublets, especially the one at 1167 kev. The well-known 873-kev resonance from F^{19} contamination can be seen in Fig. 3.

Fifty-four resonances were observed in the region investigated between 0.7 and 1.8 Mev of proton energy. The resonance energies can be found listed in Table II, discussed in Sec. III.

[4] R. O. Bondelid, Naval Research Laboratory Quarterly Report on Nuclear Science and Technology, January 1, 1957 (unpublished), p. 1.

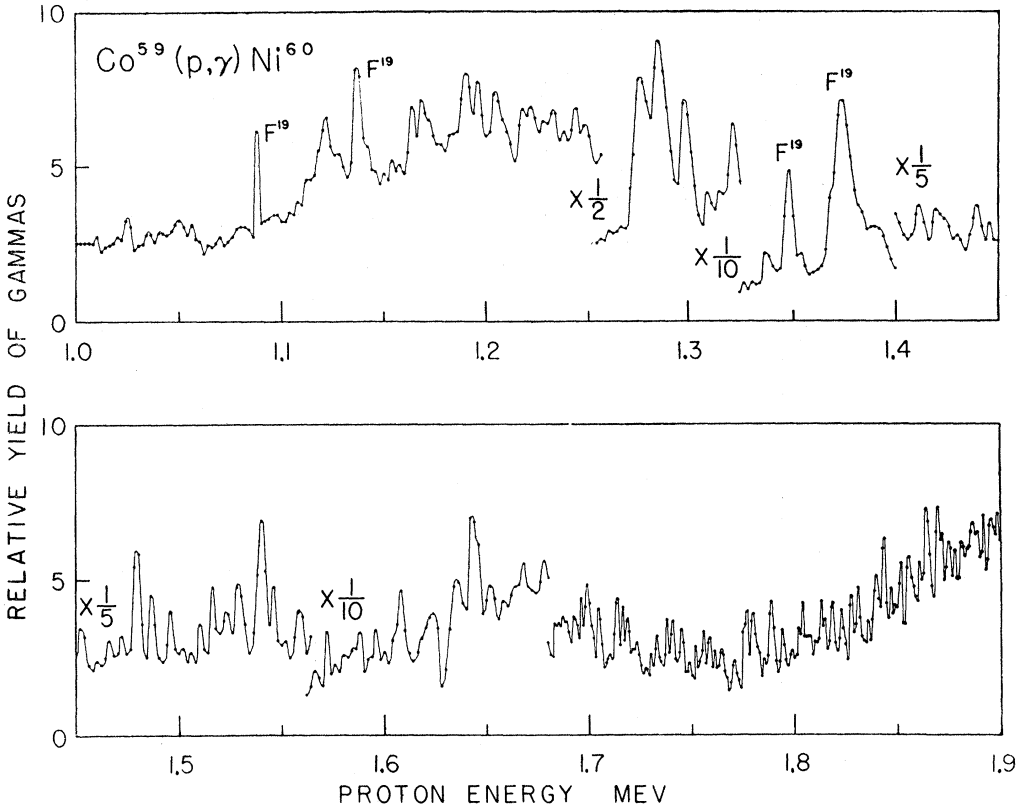

FIG. 4. Excitation function for the yield of gamma rays with energy greater than 4.5 Mev in the Co^{59}-$(p,\gamma)Ni^{60}$ reaction. Background counts have not been subtracted. The peaks marked "F^{19}" are due to the $F^{19}(p,\alpha\gamma)O^{16}$ reaction. The discontinuity at about 1.68 Mev corresponds to a change to a thinner (1 kev) target. Statistical uncertainties are of the order of the diameter of the solid circles.

$Co^{59}(p,\gamma)Ni^{60}$

Figure 4 shows a plot of the excitation curve of the $Co^{59}(p,\gamma)Ni^{60}$ reaction. Resonances due to F^{19} are so labeled. It is apparent that many resonances remain unresolved, despite the fact that over much of the region investigated, a 1-kev thick target was bombarded at 1-kev intervals of bombarding energy. Because of the large number of resonances observed, about 150, no compilation of bombarding energies at which individual resonances appear is given. It should be remarked here that the yield function cannot be considered a smoothly rising one with a rather bad scatter of the points as might be suspected from a first look at the points of Fig. 4, because the points shown were readily repeatable within the normal statistical deviation, which for much of Fig. 4 is about the diameter of the circles representing the data points.

Since numerous breaks occur in Fig. 4, occasioned by changes of scale and different targets with varying degrees of fluorine contamination and different thicknesses, the gross features of the curve are not readily apparent. For this reason the curve of Fig. 5 was obtained using a 0.52-mg/cm² target (50 kev thick to 1.5-Mev protons). The integrated effect of the resonances contained in the 50-kev interval is sufficiently great to make negligible the effects of the radiation due to the fluorine, because the fluorine from the vacuum system appears only as a thin surface contaminant on the electroplated targets. The ordinate is in millibarns (total capture cross section integrated over the entire solid angle) and represents the average cross section over the region of the target thickness. The absolute cross section was determined as described in Sec. III.

III. CROSS SECTIONS

A. Procedure

To determine absolute gamma-ray yields using NaI crystals, the following factors must be taken into

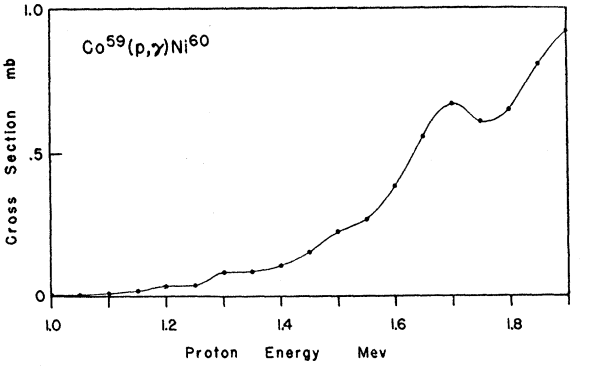

FIG. 5. Excitation function for proton capture by Co^{59}. Ordinate represents the total integrated capture cross section in units of millibarns. The target was 50 kev thick for 1.5-Mev protons. Background was negligible. Statistical uncertainties are smaller than the diameter of the solid circles.

TABLE II. For the $Ni^{60}(p,\gamma)Cu^{61}$ reaction: resonance bombarding energies (E_p), compound-nucleus excitation energies (E_x), the "thick-target" yields (for 4π steradians) of primary gamma rays, and the integrated cross sections ($\int\sigma dE$). Uncertainties are indicated below the dimension headings. The last digit of E_x has relative significance only.

E_p (kev) (±2)	E_x (Mev) (±0.03)	Yield (γ rays/μcoul) (factor of 2)	$\int\sigma dE$ (ev barns) (factor of 2)
725	5.523	6	0.01
895	5.690	5	0.01
1029	5.822	11	0.02
1066	5.859	25	0.05
1078	5.870	20	0.03
1132	5.923	25	0.04
1167	5.958	85	0.15
1197	5.987	70	0.13
1209	5.999	75	0.14
1239	6.029	70	0.13
1247	6.037	60	0.10
1313	6.102	120	0.21
1319	6.107	150	0.25
1323	6.111	180	0.29
1331	6.119	25	0.06
1343	6.131	280	0.45
1347	6.135	260	0.40
1371	6.159	90	0.15
1381	6.168	120	0.20
1415	6.202	220	0.35
1431	6.218	120	0.18
1451	6.237	600	0.75
1461	6.247	100	0.14
1465	6.251	75	0.11
1483	6.269	90	0.14
1491	6.277	90	0.14
1515	6.300	280	0.40
1519	6.304	450	0.70
1529	6.314	40	0.06
1538	6.323	250	0.35
1566	6.350	150	0.22
1577	6.361	250	0.35
1588	6.372	650	0.9
1599	6.383	1600	2.3
1605	6.389	1550	2.0
1620	6.403	1500	1.8
1639	6.422	95	0.14
1643	6.426	240	0.35
1649	6.432	210	0.29
1656	6.439	700	1.0
1669	6.452	290	0.40
1674	6.457	950	1.0
1679	6.462	350	0.50
1694	6.476	700	1.0
1698	6.480	230	0.30
1711	6.493	170	0.23
1721	6.503	80	0.11
1734	6.516	550	0.70
1739	6.521	220	0.30
1757	6.538	400	0.50
1764	6.545	450	0.60
1770	6.551	550	0.75
1783	6.564	450	0.55
1793	6.574	350	0.45

account: (1) the attenuation of the gamma rays by materials between the target and the crystal, (2) the intrinsic efficiency of the crystal, and (3) the "bias efficiency" of the counting arrangement. The manner in which each factor was handled is described in succeeding paragraphs.

The calculation of the attenuation of the gamma rays by the intervening materials was carried out by a numerical integration of the individual attenuations by each material for each incremental gamma-ray direction. All dimensions entering into this calculation were directly measurable, except the distance from the face of the crystal to the face of the containing can. Since the 3-in.×3-in. NaI crystal used for the cross section measurements was obtained already potted by the manufacturer, Harshaw Chemical Company, the crystal assembly was "gamma rayed" in the following manner.

The assembly was illuminated by Co^{60} gamma rays collimated by 8 in. of Pb. The crystal was translated across the collimator on a track having a micrometer traveling screw. The micrometer setting at which the face of the aluminum can was visually aligned with the center of the collimating slit was recorded. The crystal counting rate was also recorded as a function of micrometer setting. The midpoint of the rise in the counting-rate curve was taken as the point at which the face of the crystal itself was at the center of the slit. It was thus determined that the face of the crystal was 6.6 mm from the face of the Al can.

The intrinsic efficiency of the crystal may be found in the tables of Wolicki *et al.*[5] in terms of the crystal-face-to-source distance and the energy of the gamma ray. The over-all efficiency of the counting arrangement may then be determined as the product of the intrinsic efficiency and the "bias efficiency." We define bias efficiency as the number of pulses, of sufficient height to trigger the discriminator, divided by the total number of pulses in the crystal due to that particular gamma ray. The bias efficiency was determined experimentally for several monoenergetic gamma rays of different energies, using the same geometry as was used in observing the resonances.

The beam intensity was determined using a current integrator of the Higinbotham type[6] with the usual precautions being taken, such as the use of an electron repeller in front of the target Faraday cage.

As a check on the reliability of this method of determining gamma-ray yields, a measurement was made of the thick-target yield of the $F^{19}(p,\alpha\gamma)O^{16}$ reaction at the 873-kev resonance, and the result was compared with that of Chao *et al.*[7] Our result of 3.3 quanta per 10^7 protons was 11% lower than their result, which may be considered a standard since it was in agreement with their measurement of the coincident α-particle yield. We therefore conclude that the calculated intensity of a monoenergetic gamma ray should have an uncertainty no greater than 20%. For multiple gamma rays, where the determination of the bias efficiency is less accurate, the uncertainty might be as high as 50%.

[5] Wolicki, Jastrow, and Brooks, Naval Research Laboratory Report 4833, 1956 (unpublished).
[6] W. A. Higinbotham and S. Rankowitz, Rev. Sci. Instr. **22**, 688 (1951).
[7] Chao, Tollestrup, Fowler, and Lauritsen, Phys. Rev. **79**, 108 (1950).

For resonances observed at only one angle, a further uncertainty arises due to possible asymmetries in the gamma-ray emission. But since a rather large fraction of the total solid angle (40%) was subtended by the crystal, and since the multiplicity of gamma rays emitted from a resonant state tends to cancel part of the anisotropy of any one of the gamma rays, the integrated yield will normally be within a factor of two of that calculated assuming isotropy.

The bias was never set below one-half of the energy of the direct ground-state transition in order not to count more than one member of a cascade, in those instances where de-excitation occurred predominantly through stop-over transitions. This procedure could miss some counts where three or more gamma rays were involved in the cascade, and none of them had more than one-half of the total energy. However, after examination of detailed spectra from several resonances, as discussed and shown in Secs. V and VI, we believe that such cascades are negligible in number.

Since the resonant yields usually rose to the maximum in one interval of bombarding energy, the resonance shapes could not be determined. The observed yields were therefore the "thick-target resonance yield," $\int \sigma dE$, determined using formula (1), which was derived from familiar relationships.

$$\int \sigma dE = (A \cdot S/Q \cdot N)Y, \tag{1}$$

where A = mass number of the target nucleus, S = stopping power of target material in units of ev cm^2/g, Q = number of protons that struck the target, N = Avogadro's number, and Y = number of gamma rays emitted.

B. Results

$$Ni^{58}(p,\gamma)Cu^{59}$$

Since the relative intensities of capture gamma-ray yields from different resonances depend in general upon the angle of observation, a better measure of the relative integrated cross sections of the different resonances in the $Ni^{58}(p,\gamma)Cu^{59}$ reaction comes from the observations of the positron decay of the residual Cu^{59} nuclei. But an accurate determination of the absolute cross section from positron counting is difficult because of the unknown over-all detector efficiency. Therefore the absolute integrated cross section of the 1424-kev resonance was determined by detecting the gamma rays using the 3-in.×3-in. NaI crystal. The yields of the other resonances were then computed from their positron counting rates relative to that of the 1424-kev resonance.

The yields in captures per microcoulomb of incident protons are given in Table I for each resonance at proton energy "E_p." The integrated cross sections (integrated over both angle and energy) are given in the column under the heading "$\int \sigma dE$." The excitation energies in the compound nucleus are given under the heading "E_x." Since the Q-value measurements (Sec. IV) involved uncertainties of at least 0.02 Mev, the last digit in the E_x column has relative significance only.

$$Ni^{60}(p,\gamma)Cu^{61}$$

For most of the resonances in the $Ni^{60}(p,\gamma)Cu^{61}$ reaction, the yields were calculated assuming gamma-ray isotropy, the number coming from the excitation-curve data giving the relative yields in the forward 1.6π steradians.

For some of the more intense resonances for which angular distributions and branching ratios were measured, as described and listed in Secs. VI and VII, a more accurate determination of the capture yields was made by taking into account angular asymmetries.

Table II gives the resonance bombarding energies, excitation energies, yields, and integrated cross sections in the same manner as Table I does for the Ni^{58} reaction.

$$Co^{59}(p,\gamma)Ni^{60}$$

As was mentioned in Sec. IIE, the resonances in the $Co^{59}(p,\gamma)Ni^{60}$ reaction were too close together to be clearly resolved. Therefore, no attempt was made to determine the numbers pertaining to any particular resonance. Instead the excitation function for a weighed intermediate-thickness target (0.52 mg/cm^2) was determined, the absolute yield being calculated as in the nickel cases. The average cross section over each 50-kev interval of bombarding energy is shown in Fig. 5. Here we are dealing with σ instead of $\int \sigma dE$.

IV. Q-VALUE MEASUREMENTS

In order to determine the Q values of the three reactions studied, it was necessary to measure the energy of the ground-state gamma-ray transition or to measure the energy of each gamma ray in a cascade sequence to the ground state.

A. Procedure

Coincidence techniques were used to identify ground-state transitions. If there were no gamma rays in coincidence with the highest energy gamma ray in the spectrum, then it was assumed to be the ground-state transition. Conventional electronic coincidence circuits were employed.

For coincidence purposes, only the "total-capture peak" of the high-energy gamma ray was used. We shall define the three peaks customarily seen in the NaI spectrum of a high-energy gamma ray as the "total-capture peak," "single-escape peak," and "double-escape peak," respectively, in order of descending pulse height.

According to shell-model predictions, Cu^{59} and Cu^{61} have $\frac{3}{2}^-$ ground states which would allow $E1$ or $M1$ transitions from excited states formed from Ni^{58} or Ni^{60}

(both even, even) and s-wave or p-wave protons. Therefore, one would expect that some of the resonances would exhibit ground-state transitions.

In measuring the ground-state gamma-ray energies, the same 3-in.×3-in. NaI crystal and associated electronic equipment were used as were used for the excitation curves and cross sections. The spectrometer was calibrated with two well-known gamma rays, the 4.43-Mev gamma ray from a Po-Be source, and the 6.14-Mev gamma ray from the $F^{19}(p,\alpha\gamma)O^{16}$ reaction at the 1372-kev resonance. Thus for both the Ni^{58} and Ni^{60} measurements the energy of the unknown gamma ray was within 0.5 Mev of the energy of the calibrating gamma ray, and the difference in energy of the two gamma rays was measured in terms of the 0.511-Mev separation of the total-capture and single-escape peaks of the calibrating gamma ray. This procedure eliminated practically all of the uncertainty in calibration due to nonlinearity in the spectrometer.

Another bothersome source of possible error in calibration was the shift in gain with phototube current. In order to eliminate this gain shift between calibration and measurement, the intensity of the calibrating gamma ray was adjusted to give the same phototube current as the unknown gamma ray. The phototube current output was measured by integrating the linear amplifier output pulses. Several runs were made alternating between known and unknown gamma rays, in order to eliminate any gradual shifts in gain such as would be caused by a drifting high-voltage supply.

The Doppler shift of the gamma-ray energy due to the motion of the emitting nucleus was much smaller than the experimental uncertainties and was therefore ignored.

Since the uncertainty due to the standard statistical deviation of the counts per channel is greatest at the top of the peaks, and since the relative flatness at this point makes these uncertainties very critical in determining the exact position of the center of the peak, the center was determined by taking the midpoints between the steep sides at several places on the upper half of the peak. The position of the center could thus be found repeatedly within about ±0.1 channel. At most, the uncertainty was less than 0.1 of the full width at half-maximum.

The resolution of the complete spectrometer was about 3% for a 6-Mev gamma ray.

B. Results

$$Ni^{58}(p,\gamma)Cu^{59}$$

The Q value of the $Ni^{58}(p,\gamma)Cu^{59}$ reaction was measured for five different resonances as shown in Table III, and found to be 3.42±0.02 Mev. The 4.43-Mev gamma ray from a Po-Be source served as the energy standard. The fact that all the resonances gave the same Q value within a small uncertainty strengthens the assumption, based on coincidence studies, that the ground-state transition was being observed.

Figure 6 shows both the Cu^{59} gamma ray and the Po-Be gamma ray plotted on the same graph, taken at the 1424-kev resonance. The internal consistency as demonstrated in Table III suggests a 0.01-Mev uncertainty, but we prefer to assign an over-all uncertainty of about 0.02 Mev, which allows for some error in the energy standard, and some systematic error in the procedure.

This Q-value measurement closes the mass-excess cycle among the nuclides, Ni^{58}, Ni^{59}, and Cu^{59}. The mass-excess difference Ni^{58}-Ni^{59} has been determined by Harvey,[8] using the (d,p) reaction, to be 0.64±0.10 Mev, and by Kinsey and Bartholomew,[9] using the (n,γ) reaction, to be 0.633±0.006 Mev. The mass-excess difference Cu^{59}-Ni^{59} can be calculated from the Cu^{59} positron end point of Yuasa *et al.*[10] to be 2.87±0.05 Mev. The mass-excess difference Cu^{59}-Ni^{59} may therefore be computed to be 2.24±0.05 Mev, which is in marked disagreement with our result of 4.16±0.02 Mev, computed from our $Ni^{58}(p,\gamma)Cu^{59}$ Q value given in Table III. Concurrent with the present experiment, Prosser *et al.*[11] measured the positron end point of Cu^{59}, and if we use their value, the Cu^{59}-Ni^{59} mass-excess difference is computed to be 4.13±0.10 Mev, which is in excellent agreement with our value of 4.16±0.02 Mev.

$$Ni^{60}(p,\gamma)Cu^{61}$$

The Q value of the $Ni^{60}(p,\gamma)Cu^{61}$ reaction was measured at seven different resonances yielding the average value of 4.81±0.03 Mev. Figure 7 shows the spectra of the 6.14-Mev calibrating gamma ray from the $F^{19}(p,\alpha\gamma)O^{16}$ reaction and the Cu^{61} gamma ray from the 1620-kev resonance.

This Q value completes the mass-excess cycle, Ni^{60}-Ni^{61}-Cu^{61}. The Cu^{61}-Ni^{61} mass-excess difference can be determined from the $Cu^{61}(\beta^+)Ni^{61}$ positron end point, measured by Owen *et al.*,[12] to be 2.227±0.005

TABLE III. Summary of ground-state transition energy measurements for the $Ni^{58}(p,\gamma)Cu^{59}$ reaction.

E_p (kev)	$E\gamma$ (Mev)	Q (Mev)
1100	4.49	3.41
1308	4.70	3.42
1424	4.82	3.42
1716	5.10	3.42
1844	5.24	3.43
	av Q=3.42±0.02	

[8] J. A. Harvey, Phys. Rev. **81**, 353 (1951).
[9] B. B. Kinsey and G. A. Bartholomew, Phys. Rev. **89**, 375 (1953).
[10] Yuasa, Nahmias, and Vivargent, J. phys. radium **16**, 654 (1955).
[11] Prosser, Moore, and Schiffer, Bull. Am. Phys. Soc. Ser. II, **1**, 163 (1956).
[12] Owen, Cook, and Owen, Phys. Rev. **78**, 686 (1950).

Mev. The Ni^{61}-Ni^{60} mass-excess difference was measured by Collins *et al.*,[13] using a mass spectrometer, to be 0.06 ± 0.34 Mev, and by Hoesterey,[14] using the (d,p) reaction, to be -0.16 ± 0.04 Mev, and by Kinsey and Bartholomew,[9] using the (n,γ) reaction, to be -0.168 ± 0.009 Mev. Using these values, the mass-excess difference Cu^{61}-Ni^{60} may be computed to be 2.059 ± 0.010 Mev, which may be compared with our result of 2.77 ± 0.03 Mev. This discrepancy of 0.71 Mev is more than 20 times the square root of the sum of the squares of the individual uncertainties, and therefore cannot be tolerated.

In order to clarify this situation, and to bring order to the considerable confusion surrounding the level structures of the nuclides involved, two additional studies were carried out in this laboratory.[15,16] From the results of these studies and from a detailed examination of Hoesterey's thesis,[14] it appears that Hoesterey assigned some proton groups from the (d,p) reactions to the wrong isotopes. When we made isotopic reassignments of Hoesterey's proton groups, and made corresponding reassignments of the gamma rays of Kinsey and Bartholomew,[9] their gamma-ray D became the ground-state transition from neutron capture by Ni^{60}. Using this new value of the (n,γ) Q value, the computed Cu^{61}-Ni^{60} mass-excess difference becomes 2.774 ± 0.010 Mev, which is in excellent agreement with our value of 2.77 ± 0.03 Mev.

After the present experiment was finished, a new table of mass-spectrometer masses was published by Quisenberry *et al.*[17] Their masses for the nickel isotopes are in considerable disagreement with the older mass-spectrometer values,[13] but are in good agreement with the present (p,γ) Q values.

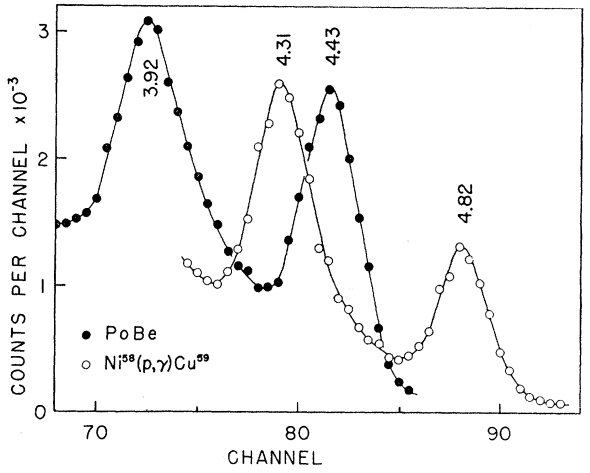

FIG. 6. High-energy portion of spectrum of gamma rays from the 1424-kev resonance in the $Ni^{58}(p,\gamma)Cu^{59}$ reaction (open circles) and the Po-Be gamma ray (solid circles). The Q value of the reaction was determined from the measurement of the ground-state gamma ray (highest energy peak).

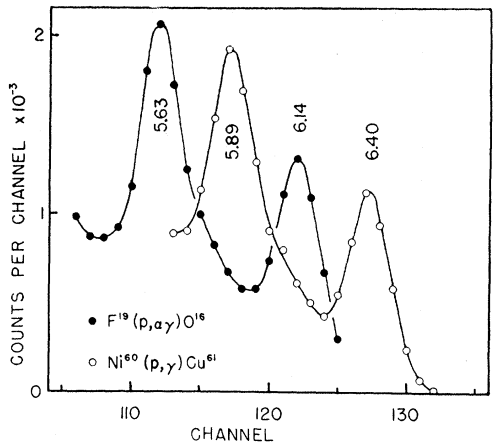

FIG. 7. High-energy portion of spectrum of gamma rays from the 1620-kev resonance in the $Ni^{60}(p,\gamma)Cu^{61}$ reaction (open circles) and the gamma ray from the $F^{19}(p,\alpha\gamma)O^{16}$ reaction at the 1372-kev resonance (solid circles). The Q value of the reaction was determined from the measurement of the ground-state gamma ray (highest energy peak).

$$Co^{59}(p,\gamma)Ni^{60}$$

As was mentioned in Sec. I, the $Co^{59}(p,\gamma)Ni^{60}$ reaction was unlike the two nickel reactions in several respects. From a consideration of spins and parities, it was not surprising that the direct ground-state transition was not observed. Because of this fact, and because the Q value of this reaction could be accurately calculated from reliable information from other experiments,[18,19] a precise measurement was not attempted. However, the measurements were accurate enough to allow positive identification of the higher energy peaks with certain well-known low-lying levels in Ni^{60}, as will be seen later in Sec. V.

V. CASCADE GAMMA RAYS

In general, excited states formed by resonant proton capture may be expected to decay sometimes to lower excited states as well as to the ground state of the residual nucleus. Thus it is possible to detect low-lying excited states of the compound nucleus by observing either of the following: (1) high-energy gamma rays with less energy than the ground-state transition, and (2) low-energy gamma rays in coincidence with the higher energy counterparts.

A. Procedure

Because of other low-energy radiation present, such as the nuclear gamma rays following positron decay,

[13] Collins, Nier, and Johnson, Phys. Rev. **86**, 408 (1952).
[14] D. C. Hoesterey, Ph.D. thesis, Yale University, 1952 (unpublished); verbal report, Phys. Rev. **87**, 216(A) (1952); quoted in Nuclear Science Abstracts **6**, No. 24B, 19 and 50 (1952).
[15] Butler, Dunning, and Bondelid, Bull. Am. Phys. Soc. Ser. II, **1**, 327 (1956).
[16] Butler, Gossett, and Holmgren, Bull. Am. Phys. Soc. Ser. II, **1**, 163 (1956).
[17] Quisenberry, Scolman, and Nier, Phys. Rev. **104**, 461 (1956).
[18] G. M. Foglesong and D. G. Foxwell, Phys. Rev. **96**, 1001 (1954).
[19] R. W. King, Revs. Modern Phys. **26**, 327 (1954).

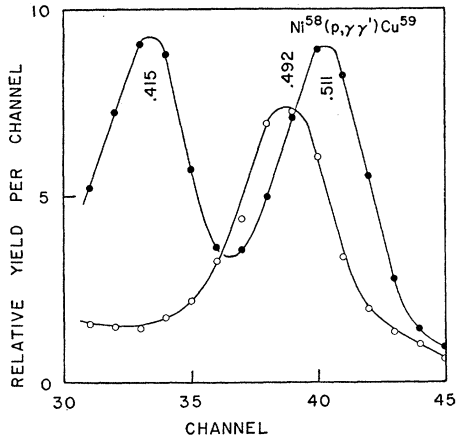

FIG. 8. Portion of spectrum of gamma rays in coincidence with other gamma rays from 2.0 to 5.5 Mev from the $Ni^{58}(p,\gamma\gamma')Cu^{59}$ reaction (open circles) and the corresponding ungated spectrum (solid circles). The two peaks in the ungated spectrum correspond to positron annihilation radiation and Coulomb-excitation gamma rays from the silver target backing. The ordinate scales are different for the two curves.

the annihilation radiation, and the Coulomb-excitation gamma rays from the silver target backing, direct measurements on the low-energy cascade gamma rays were not possible. It was necessary to "gate" the low-energy spectrometer with a pulse from another spectrometer set to be triggered by the corresponding high-energy transition. For these measurements the high-energy spectrometer included a 3-in.×3-in. crystal, and the low-energy spectrometer included either a 3-in.×3-in. crystal or a $1\frac{1}{2}$-in. diameter×1-in. long crystal. In order to avoid radiation scattered from one crystal to the other, a 1-in. thick Pb block was placed between the two crystals.

In a number of cases, it was possible to find a high-energy gamma ray and a low-energy gamma ray whose sum equaled to the ground-state transition. In general, one would expect that the high-energy member of the pair was emitted first because of the energy dependence of partial gamma-ray widths, and that therefore the low-energy gamma ray was emitted by an excited state of the same energy. This rule is not always valid; however, in the experiments described herein, the high-energy member was emitted first in all cases where both members of a pair were identified. This is evident because the low-energy member retained the same energy for the different resonances, whereas the high-energy member changed its energy directly with the resonance energy in the center-of-mass system. Therefore, we have assigned an excited state to each low-energy member of all such pairs identified.

The identification of the high-energy member of a cascade was complicated by the intrinsic response of NaI crystal spectrometers to such gamma rays, because each high-energy gamma ray gives rise to three peaks. In analyzing the high-energy part of a complicated spectrum, it is sometimes helpful to take the spectrum using two crystals of different size. The response of a 3-in.×3-in. crystal emphasizes the single-escape peak, and depresses the double-escape peak, while the $1\frac{1}{2}$-in. ×1-in. crystal emphasizes the double-escape peak, and has almost no total-capture peak. Thus by comparing the same spectrum of gamma rays using the two crystals, certain peaks in a complicated spectrum could be labeled as double-escape or total-capture.

B. Results

$Ni^{58}(p,\gamma\gamma')Cu^{59}$

The low-energy gamma rays in coincidence with gamma rays from 2.0 to 5.5 Mev are listed in Table IV, with their respective uncertainties in energy measurement. To conserve space, only one of the low-energy gamma-ray peaks is illustrated. The one picked for illustration, 0.492 Mev, was so chosen because it was the most difficult to isolate and identify for two reasons. (1) Its energy is very close to that of the annihilation radiation from the positron decay of the Cu^{59} formed in the reaction, and this annihilation radiation is known[11,16] to be in coincidence with nuclear gamma rays up to about 2 Mev from the Ni^{59} following beta decay. (2) Its energy is very close to that of the annihilation radiation formed by the decay of the positron of the pair created by the high-energy gamma ray in the "gate" crystal, and which might have scattered into the low-energy crystal, and would of course be in true coincidence.

The open circles of Fig. 8 give the coincidence spectrum in the low-energy crystal. The closed circles show the ungated spectrum, including the 0.511-Mev peak from the annihilation radiation, and the 0.415-Mev peak from the Coulomb excitation of the silver target backing. The data for Fig. 8 were taken at the 1424-kev resonance, with the coincidence gate set from 2.0 to 5.0 Mev.

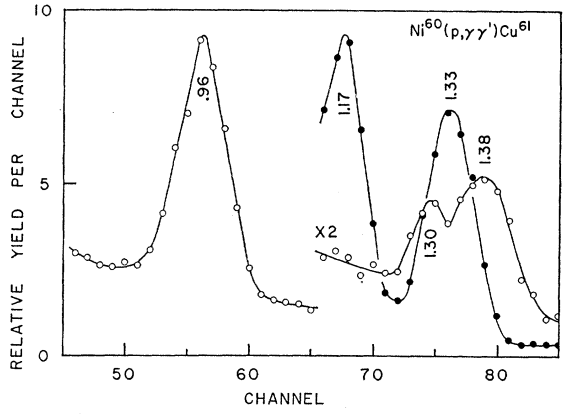

FIG. 9. Portion of spectrum of gamma rays in coincidence with other gamma rays from 4.5 to 6.5 Mev from the $Ni^{60}(p,\gamma\gamma')Cu^{61}$ reaction (open circles) and the Co^{60} source spectrum used for calibration purposes (closed circles).

$Ni^{60}(p,\gamma\gamma')Cu^{61}$

The low-energy gamma rays in coincidence with radiation from 4.5 to 6.5 Mev are also listed in Table IV. Again, in order to conserve space, only a part of the coincidence spectrum is shown, and that is the part most difficult to interpret. The 0.96-Mev gamma ray shown in Fig. 9 is straightforward, but the doublet, 1.30 and 1.38-Mev, suggests the possibility of a state 80 kev above the ground state. A search for an 80-kev gamma ray in coincidence with the high-energy radiation yielded inconclusive results. So the suggestion remains only a possibility.

$Co^{59}(p,\gamma\gamma')Ni^{60}$

The low-energy cascade gamma rays, also listed in Table IV, are not illustrated in order to conserve space, but the high-energy portion of the gamma-ray spectrum is shown in Fig. 10. In order to identify the spectrum peaks in terms of gamma-ray energies, two crystals of different size were used, 3-in.×3-in. and 1½-in.×1-in.,

TABLE IV. Low-energy cascade gamma rays found in coincidence with capture radiation between the energy limits listed as the "gate."

$Ni^{58}(p,\gamma\gamma')Cu^{59}$ Gate: 2–5.5 Mev (Mev)	$Ni^{60}(p,\gamma\gamma')Cu^{61}$ Gate: 4.5–6.5 Mev (Mev)	$Co^{59}(p,\gamma\gamma')Ni^{60}$ Gate: 6–11 Mev (Mev)
0.492±0.005	0.468±0.01	0.47±0.02
0.908±0.02	0.96 ±0.02	0.84±0.02
1.38 ±0.03	1.30 ±0.02	0.95±0.02
1.78 ±0.02	1.38 ±0.02	1.07±0.02
2.00 ±0.04	1.63 ±0.03	1.17 cal.
2.32 ±0.04	1.91 ±0.03	1.33 cal.
		1.64±0.03
		1.77±0.03

as discussed in Sec. VA. The response of the two crystals to the monoenergetic 4.43-Mev radiation from a Po-Be source is shown in channels 31 to 50. The spectrum from the Co^{59} reaction using a 2-kev thick target and a bombarding energy of 1.9 Mev is shown in channels 70 to 115. From the response of the two crystals, the peaks were assigned to gamma-ray energies, and hence to particular cascades, and are so labeled. The abbreviations stand for total-capture, single-escape, and double-escape. The numbers represent the energy of the state through which the particular cascade occurs. Spectra obtained at other bombarding energies (not illustrated) showed evidence of decay to the 2.16-, 3.59-, and 3.9-Mev states of Ni^{60} as well as to those which appear in the spectra of Fig. 10.

The low-energy coincident gamma rays have been assigned to particular levels of Ni^{60}. It was not possible to fit all of the gamma rays to the level scheme[20] that

[20] *Nuclear Level Schemes, A=40—A=92,* compiled by Way, King, McGinnis, and van Lieshout, Atomic Energy Commission Report TID-5300 (U. S. Government Printing Office, Washington, D. C., 1955).

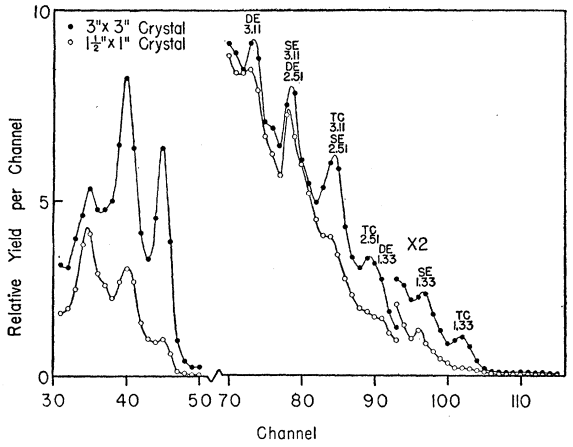

FIG. 10. Spectra of gamma rays from the $Co^{59}(p,\gamma)Ni^{60}$ reaction using two crystals of different size. Channels 31 to 50 illustrate the response of the two crystals to the 4.43-Mev gamma ray from a Po-Be source. Channels 70 to 115 show the spectra of high-energy capture gamma rays. The three peaks associated with each gamma-ray energy are labeled TC, SE, and DE to represent total-capture, single-escape, and double-escape, respectively. Each peak is also marked with the energy of the excited state involved in the cascade.

was known at the time the data were taken. However, with the additional levels in Ni^{60} found by Paris and Buechner,[21] it has been possible to fit all of the observed low-energy cascade gamma rays to particular levels as shown in Fig. 11. In making these assignments, both the high-energy primary gamma ray and its low-energy counterpart were reasonably well identified. Because of the close spacing of levels in the vicinity of 4 Mev, some ambiguity does exist in the assignment of the 1.64-Mev secondary gamma ray. The assignment shown gives an excellent fit with respect to the difference in

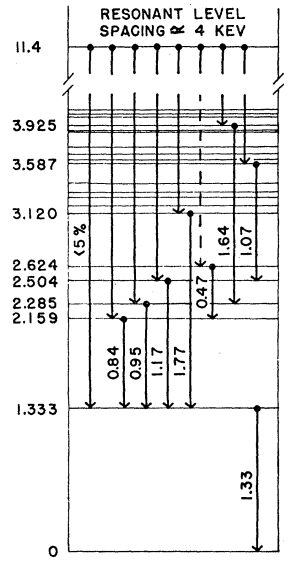

FIG. 11. The assignment of gamma rays from the $Co^{59}(p,\gamma\gamma')Ni^{60}$ reaction to levels in Ni^{60}. Some of the upper levels are so closely spaced that only the ones of interest are labeled. The energy values shown for the transitions are the direct measurements of the present experiment. The levels of Ni^{60} are those of Paris and Buechner.

[21] C. H. Paris and W. W. Buechner, Bull. Am. Phys. Soc. Ser. II, 2, 61 (1957); verbal report.

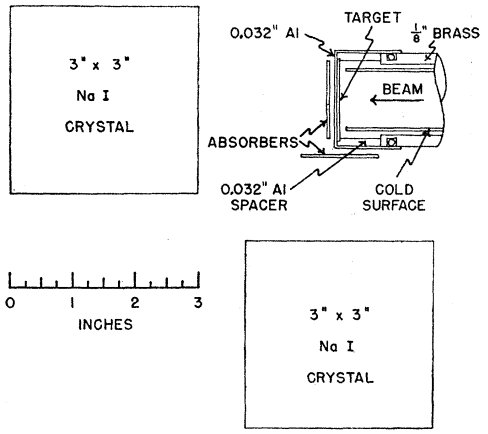

FIG. 12. The geometrical arrangement of the two crystals used in determining the branching ratios. The absorbers attenuated the silver x-rays and Coulomb-excitation gamma rays. The attenuation, by the target backing and holder, of the gamma rays emitted in the direction of the 90° crystal was about 1%.

energy between the two levels, and a high-energy primary gamma ray feeding a level in the vicinity of 3.9–4.0 Mev was observed. The energy values shown on the transitions are the direct measurements of the present experiment.

The decay scheme of Fig. 11 is not complete because no search was made for cascade gamma rays above 2 Mev. Thus the absence of ground-state-transition indications for states above 2 Mev does not mean that such transitions do not occur.

VI. BRANCHING RATIOS

The purpose of obtaining branching ratios was twofold. (1) It would establish with reasonable certainty which of the low-energy cascade gamma rays corresponded to states of the same energy. (2) It would enable one to obtain the relative transition probabilities of the gamma rays to the several low-lying states.

A. Procedure

Figure 12 shows the geometrical arrangement of the detectors used to determine the branching ratios of the gamma-ray transitions from some of the more intense resonances. It is not customary in such measurements to have the plane of the target backing material at 90° with respect to the beam. However, for the high-energy gamma rays under investigation, and for the relatively large crystal solid angle, the attenuation of the gamma rays emitted in the direction of the 90° crystal was at most 1%, and correction was made for this effect. The absorbers consisted of a sandwich of 0.005 in. of molybdenum to absorb the silver x-rays, and 0.020 in. of gold to attenuate the intense Coulomb excitation gamma rays from the silver backing.

The light outputs of the two crystals were sorted by two 20-channel analyzers. The yield of each particular gamma ray was obtained by taking the yields at 0° and 90° obtained by the two crystals of Fig. 12, and integrating this yield over 4π solid angle assuming a straight-line angular distribution between the two values at 0° and 90°. Because of the relatively large solid angle subtended by each crystal, this straight-line assumption introduces an error of less than 5%. The limit of error introduced was determined by integrating over 4π solid angle using some of the actual angular distributions obtained for the ground-state transitions from some of the resonances (see Sec. VII).

In order to determine the yield of the gamma ray of each particular energy, it was necessary to subtract the spectrum of the highest energy gamma ray from the total spectrum, then subtract the spectrum of the next highest energy gamma ray, etc. Before this could be done, however, it was necessary to determine the response of the crystal to monoenergetic gamma rays of several energies, using the same geometry as that of Fig. 12. This was done by determining the spectrum of several monoenergetic gamma-ray sources from about 3 Mev to about 6 Mev.

The same corrections were applied to the branching-ratio spectra as were applied to the cross-section measurements. The over-all uncertainties in the branching ratios are about 10% of the total yield from the resonance.

B. Results

$Ni^{58}(p,\gamma)Cu^{59}$

The branching ratios from five different resonances were determined and are shown in Table V. The spectra from the 0° crystal are shown in Fig. 13. The information in Table V establishes reasonably well that all of the low-energy cascade gamma rays correspond to states of the same energy, with the exception of the 1.38-Mev gamma ray, whose branching ratio in any of the listed cascade schemes did not exceed 10%, which is equal to the uncertainty involved. Since its energy is apparently not equal to the difference in energy between any other two gamma rays, it is tentatively listed as a state. It could conceivably be relatively intense in the cascade schemes for some of the weaker resonances.

The measurements of transitions to states at 2.00 and 2.32 Mev were not so reliable as for the lower

TABLE V. Branching ratios (%) from certain resonances in the $Ni^{58}(p,\gamma)Cu^{59}$ reaction at proton energies E_p (kev) to the excited states E_x (Mev). Uncertainties are ±10% of the total gamma-ray intensity.

E_p \ E_x	0	0.492	0.908	1.38	1.78	2.00	2.32
1376	5	35	20	10	0	15	15
1424	35	50	0	10	0	0	5
1663	10	5	35	0	25	15	10
1716	65	0	30	0	0	0	5
1844	95	0	0	0	0	0	5

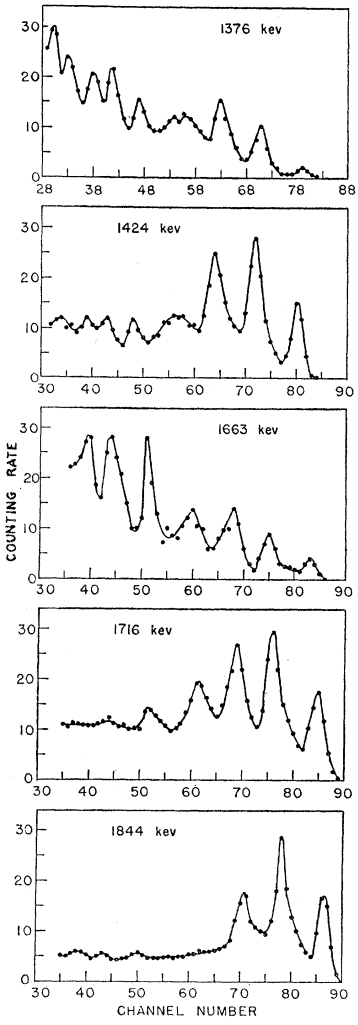

FIG 13. The spectra observed in the 0° crystal from five of the most intense resonances in the $Ni^{58}(p,\gamma)Cu^{59}$ reaction. The proton energies at resonance are shown.

states. However, in several instances involving these states, the other member of the pair could be found as illustrated in the spectra of Fig. 13.

$$Ni^{60}(p,\gamma)Cu^{61}$$

Ten different resonances were investigated giving the results shown in Table VI. The spectra from the 0° crystal are shown in Fig. 14. Only one resonance showed a definite transition to the 0.468-Mev state (the 1656-kev resonance), but several resonances gave indications of about 10% yield to the 0.468-Mev state. Likewise, transitions to the 0.96-Mev state were relatively weak. Since only one of the ten resonances studied in detail showed any indication of a transition to a 1.63-Mev state, and that indication is very weak (within the experimental error), it is possible that the 1.63-Mev gamma ray is a member of a triple cascade. However, since the ten resonances studied in detail were not chosen at random, but were the most intense of the resonances, they have a certain amount of homogeneity, and therefore might as a group discriminate against a particular transition. The 1.63-Mev gamma ray apparently does not equal the difference in energy between any other two gamma rays and is therefore tentatively assumed to come from a state of the same energy.

As in the Ni^{58} case, transitions to states above about 1.9 Mev could not be reliably measured. However, there were fairly definite indications of states at about 2.4 and 2.9 Mev, since both members of a pair could sometimes be identified from the spectra of Fig. 14.

VII. ANGULAR DISTRIBUTIONS

In order to determine the angular momenta of the compound states giving rise to several of the most intense resonances, angular distribution measurements were taken on the most energetic gamma ray emitted in each of these cases. In all cases except one (the 1376-kev resonance of Ni^{58}) this was the ground-state transition.

A. Experimental Procedure

Two NaI crystals, each 3 in.×3 in. were used in determining the angular distributions. The detector geometry was conventional, and is therefore not illustrated. One crystal was fixed at 90° at a distance of $1\frac{1}{2}$ in. from the target. The other crystal was rotated on an arc of radius $5\frac{5}{8}$ in. about a vertical axis through the target. We choose as the criteron of angular resolution the angle between the central ray (axis of the crystal) and a ray to the centroid of the volume of the crystal on each side of the central ray. This angle was 5°. No correction was made for the angular resolution of the detector because in all cases, the error introduced by the finite size of the detector was less than the statistical uncertainty in the number of counts. Corrections were made, however, for the unequal absorption of the gamma rays by the material around the target, including the 0.010-in. Ag target backing. These corrections were at most 2%.

The fixed crystal was used as a monitor. Since the data for each angle sometimes required up to one hour, making a run of six angles about six hours, the stability

TABLE VI. Branching ratios (%) from certain resonances in the $Ni^{60}(p,\gamma)Cu^{61}$ reaction at proton energies E_p (kev) to the excited states E_x (Mev). Uncertainties are ±10% of the total gamma-ray intensity.

E_p \ E_x	0	0.468	0.96	1.38	1.63	1.91	2.4	2.9
1451	100	0	0	0	0	0	0	0
1538	70	0	0	0	10	10	10	0
1588	25	15	10	10	0	10	10	20
1599	25	10	10	30	0	0	10	15
1605	70	0	0	20	0	0	5	5
1620	70	0	0	20	0	0	0	10
1656	80	20	0	0	0	0	0	0
1674	0	0	20	50	0	10	10	10
1694	55	10	20	0	0	0	0	15
1734	40	0	10	10	0	15	10	15

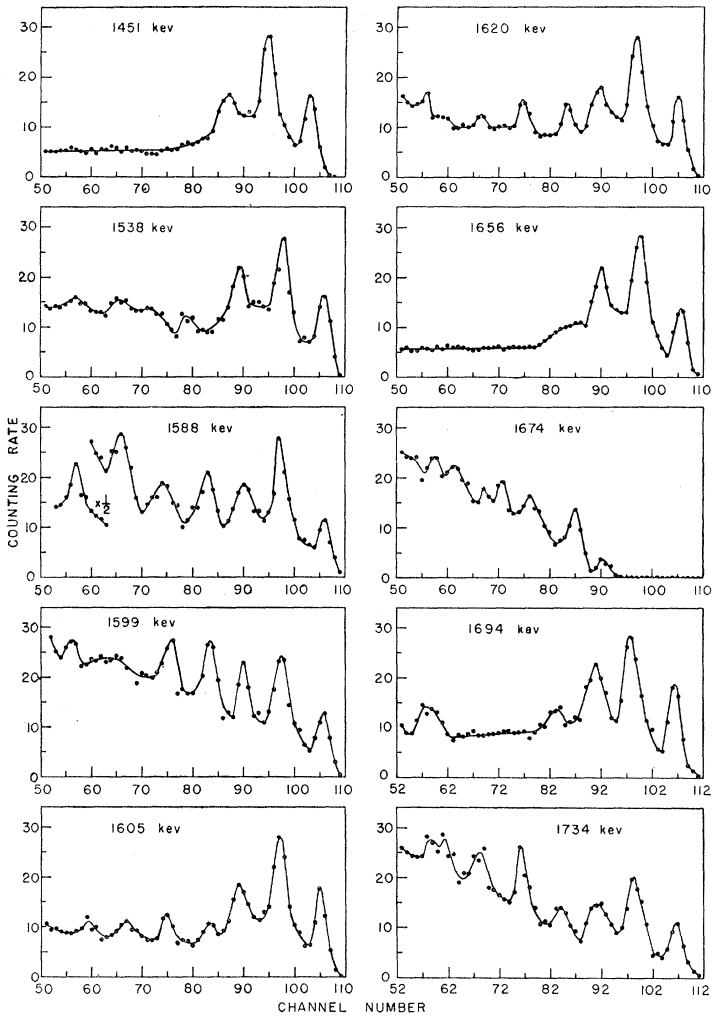

FIG. 14 The spectra observed in the 0° crystal from ten of the most intense resonances in the $Ni^{60}(p,\gamma)Cu^{61}$ reaction. The proton energies at resonance are shown.

of the gain of the monitor, as well as the movable detector, was very critical, and we were unable to achieve complete gain stability. Of the factors which determine gain stability (phototube high voltage, dynode efficiency, preamplifier gain, linear amplifier gain, and analyzer calibration) the most serious trouble seemed to come from the phototube dynode efficiency. The gain shift with counting rate seemed to approach equilibrium as if it had several different "half-lives," ranging from a few seconds to several hours.

If a narrow window were used for the monitor counts, a small percentage change in gain would cause a higher percentage change in the counting rate because more counts would be pushed out of the window than were pushed into it, or vice versa. A glance at the spectra of Figs. 13 and 14 indicates this. A wide window decreases the relative effect of gain shifts, and a wide window can be used even though it includes other gamma rays than the one whose angular distribution is being determined, because the monitor crystal's position was fixed. But even a wide window allowed appreciable errors (sometimes 5% or more, depending upon the spectral shape) for small gain shifts (1% or less).

In order to overcome the difficulties caused by gain instability, the monitor crystal output was analyzed with a 20-channel analyzer. Shifts in positions of the peaks could then be utilized to correct the data for gain changes.

The movable crystal output was likewise analyzed with another 20-channel analyzer, the only the area under the total-capture peak was used to determine the intensity of the most energetic gamma ray. Since the first excited state of both the residual nuclides, Cu^{59} and Cu^{61}, was about 500 kev (see Sec. V), the total-capture peak for a cascade to this state was included in the single-escape peak for the ground-state transition.

At each angle, counts were taken "on" resonance and "off" resonance. The off-resonance counts were subtracted from the on-resonance counts to determine the net resonance yield. Since the proton energy was changed only 2 kev from "off" to "on" resonance,

background effects were assumed to be the same for the two different energies. The off-resonance yield was usually quite small, ranging from less than 1% for the most intense resonances to a few percent for the weaker ones.

Since each resonance chosen for angular distribution measurements was well separated from the others, only one state of the compound nucleus was excited each time, and therefore the distributions should be symmetrical about 90°. The yield at 120° was obtained in each case primarily as a test of the equipment and procedure.

Interference between adjacent resonances was neglected because of the narrowness of the resonances. Resonance widths will be discussed in Sec. VIII.

B. Analysis Procedure

In comparing the experimental curves with the theory, the zero spins of the two target nuclides, Ni^{58} and Ni^{60}, allowed two simplifications. (1) Only one entrance channel spin was possible, namely that of the proton, $\frac{1}{2}$. Thus the arbitrary parameter introduced in the general case by the mixing of incoming channel spins did not occur. (2) Only one value of the orbital angular momentum, l, could contribute to any one resonance because adjacent l values have opposite parity, and l values differing by 2 or more units cannot give the same J value for the compound state. Thus another arbitrary parameter which enters in the general case, did not occur.

The maximum proton angular momentum to be considered is limited by the multipolarity of the emitted gamma ray. For protons with $l \geqslant 4$, $E1$, $M1$, and $E2$ transitions to the ground state are not possible. It is very unlikely that the resonances chosen for angular distribution measurements, the more intense ones, should be forbidden to emit $E1$, $M1$, or $E2$ radiation.

For pure lowest-multipole transitions, only 4 different distributions, W, are possible. Using the tables of Biedenharn and Rose,[22] they are as follows, in terms of the Legendre polynomials P_n with $\cos\theta$ as argument.

$$\begin{aligned}
&l=0,1 \quad && J=\tfrac{1}{2} && W=P_0,\\
&l=1,2 && J=\tfrac{3}{2} && W=P_0+0.40P_2,\\
&l=2,3 && J=\tfrac{5}{2} && W=P_0-0.40P_2,\\
&l=3 && J=\tfrac{7}{2} && W=P_0+0.510P_2-0.368P_4.
\end{aligned}$$

For a 1.6-Mev proton, the relative barrier transmission coefficients, T_l, are as follows. (For information concerning the computation of T_l, see Sec. VIII.)

$$\begin{aligned}
T_0&=1.7\times10^{-4}, & T_2&=0.12\times10^{-4},\\
T_1&=0.7\times10^{-4}, & T_3&=0.012\times10^{-4}.
\end{aligned}$$

[22] L. C. Biedenharn and M. E. Rose, Revs. Modern Phys. **25**, 729 (1953).

The symbol T_l for transmission coefficient is used instead of P_l for penetration coefficient in order to avoid confusion with the Legendre polynomials, P_n.

It will be shown later, in Sec. VIII, that the partial proton widths are probably less than the partial gamma-ray widths for proton energies less than about 1.3 Mev. Therefore, the observed intensities of the resonances below 1.3 Mev are proportional to the partial proton widths, which are in turn proportional to the barrier transmission coefficients. Since T_3 for a 1.9-Mev proton (6×10^{-6}) is less than T_0 for a 1.3-Mev proton (2×10^{-5}), it is unlikely that any of the most intense resonances chosen for angular distribution measurements were formed with $l=3$ protons. We are therefore restricted to the first three angular distributions listed above.

Some mixing of the next higher multipole is to be expected, especially when the lowest possible multipole is the magnetic type. Thus we do have one arbitrary parameter (the percentage of the next higher multipole) for fitting theoretical curves to the data. The interference phase angles were chosen following the same convention as Biedenharn and Rose.[22]

In principle, one cannot determine parity from an angular distribution, except when both target nucleus and projectile have zero spin and known parity. However in practice, one can sometimes obtain indications of parity from angular distributions involving protons and a zero-spin target nucleus. In particular, one expects that if the lowest allowed gamma-ray multipolarity is of the electric type, it will be essentially pure. But if it is of the magnetic type, observable mixing with the next higher electric multipole will sometimes occur. Thus if the experimental data can be fitted only by assuming significant admixtures (several percent or more) of the next higher multipole, there is some indication that the lowest allowed multipole is magnetic, which is in turn an indication of the parity of the emitting state.

Cascade schemes also give clues to the parity of a state. It should be emphasized that these indications of parity should be used with great care because exceptions to these rules do occur, especially transitions explained by the collective model. But since we are near the shell-closure number 28, shell model phenomena are expected to prevail. These considerations have been used together with arguments based on $E1$ and $M1$ transition rates (see Sec. VIII) to assign probable parities to some of the resonant compound states.

C. Results

$Ni^{58}(p,\gamma)Cu^{59}$

Angular distribution measurements were made on the four most intense resonances in the $Ni^{58}(p,\gamma)Cu^{59}$ reaction, and are shown in Fig. 15. The uncertainty bars on the data points indicate only the standard statistical deviation in the number of counts. Other

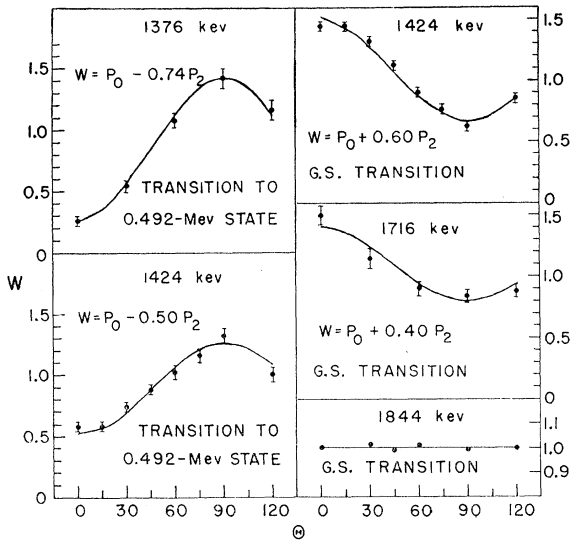

FIG. 15. The angular distributions of gamma rays from four of the resonances in the $Ni^{58}(p,\gamma)Cu^{59}$ reaction. The curves represent the equation shown in each plot. Note the displaced zero for the ordinate scale in the case of the 1844-kev resonance. The proton energies and gamma-ray transitions are labeled.

errors are believed to be smaller than the statistical uncertainty. The solid curves shown in Fig. 15, are the best visual fit to the data using the zero-order and second-order Legendre polynomials.

Since the discussion of the 1376-kev resonance depends on the prior discussion of the 1424-kev resonance, the individual resonances will be discussed from the highest energy down. Only one of the resonances (1844 kev) allowed the possibility of being excited by s-wave protons. Even it could have been excited by p-wave protons because its isotropic angular distribution indicates a spin of $\frac{1}{2}$ for the compound state, but gives no indication of the parity. The maximum deviation from a horizontal straight line was 1%, and the standard statistical deviation in the number of counts at each point was about 1%. The ground-state transition is either $M1$ or $E1$ with an indeterminate amount of $E2$ or $M2$.

An isotropic distribution could be the result of interference between different multipoles even if the compound state had a spin greater than $\frac{1}{2}$. For the present situation, the distribution would be isotropic if $J=\frac{3}{2}$, and the intensity of the quadrupole radiation was 6.7% of the dipole radiation with a phase angle of 0°. It is unlikely that such a particular set of circumstances would be encountered.

In some of the cases involving interference between dipole and quadrupole radiation, a given angular distribution can be obtained by assuming either a small amount (~1%) of quadrupole radiation mixing with predominantly dipole radiation or vice versa. In general, the small amount of dipole admixture necessary to account for the given distribution is different from (usually more than) the small amount of quadrupole admixture assumed in the former case, and the phase angles usually are different by 180°. Because of the greater emission probability of dipole radiation than quadrupole radiation for nuclides in the region which includes the ones investigated in the present experiment, the assumption of a small amount of dipole radiation will not be made.

The 1716-kev resonance showed a distribution represented by $W=P_0+(0.40\pm0.04)P_2$, which is characteristic of a spin of $\frac{3}{2}$ for the compound state, and pure dipole radiation to the ground state (<2.6% quadrupole radiation with either phase angle).

The 1424-kev resonance showed a distribution represented by $W=P_0+(0.60\pm0.04)P_2$, which also indicates a spin of $\frac{3}{2}$ for the compound state, but with an admixture of 1.7±0.7% quadrupole radiation with a phase angle of 180°.

Since the 1424-kev resonance showed approximately equal transition probabilities to the ground state and first excited state at 0.492 Mev, it was possible to determine the angular distribution of the gamma ray to the first excited state as well as to the ground state. Since the ground-state angular distribution yielded a unique determination of the spin of the compound state, the angular distribution of the gamma ray to the 0.492-Mev state yielded a unique determination of the first excited state spin. The distribution to the 0.492-Mev state shown in Fig. 15 is represented by $W=P_0-(0.50\pm0.05)P_2$ which indicates a spin of $\frac{1}{2}$ for the 0.492-Mev state and pure dipole radiation (<0.1% quadrupole admixture).

Since the 1376-kev resonance showed only about 5% transition probability to the ground state, a determination of the ground-state distribution was impractical. It was determined, however, during the branching ratio measurements that the yield at 90° was less than at 0° by roughly a factor of 2. Such a distribution is consistent with a spin of $\frac{3}{2}$ for the compound state.

Since the spin of the 0.492-Mev state was determined from the 1424-kev resonance, and since the 1376-kev resonance had a transition probability of about 35% to the first excited state, the spin of the compound state could be uniquely determined from the distribution of the gamma rays to the first excited state. This distribution can be represented by $W=P_0-(0.74\pm0.06)P_2$ as shown in Fig. 15, indicating a spin of $\frac{3}{2}$ for the compound state and an admixture of 2.3±0.7% quadrupole radiation with a phase angle of 0°.

Angular distribution measurements were also made for the 1663-kev resonance (not shown), but with a fairly large standard statistical deviation, ±15%. The distribution was isotropic within the uncertainty indicating a probable spin of $\frac{1}{2}$ for the compound state.

$$Ni^{60}(p,\gamma)Cu^{61}$$

Eight angular distributions were made and are shown in Fig. 16. Three of the distributions, at 1451, 1538,

and 1656 kev, were isotropic and therefore indicate a spin of $\frac{1}{2}$ for the compound states. Note the displaced zeros on the ordinate scale for these distributions as shown in Fig. 16.

The 1656-kev resonance could also be represented by $W=P_0+0.06P_2$ which is consistent with $J=\frac{3}{2}$ and 5% admixture of quadrupole radiation with a phase angle of 0°. The more reasonable interpretation is however an isotropic distribution indicating $J=\frac{1}{2}$.

Three other resonances at 1588, 1605, and 1694 kev, had distributions represented by $W=P_0+0.40P_2$ with uncertainties in the P_2 coefficient of ±0.08, ±0.04, and ±0.06, respectively. The compound states have a spin of $\frac{3}{2}$ and emit essentially pure dipole radiation with upper limits on the quadrupole admixture of 0.3%, 0.1%, and 0.2%, respectively.

The 1599-kev resonance had a distribution represented by $W=P_0+(0.30\pm0.05)P_2$ which indicates a spin of $\frac{3}{2}$ and 0.1% to 1% admixture of quadrupole radiation with a phase angle of 0°.

The 1620-kev resonance had a distribution represented by $W=P_0+(0.25\pm0.05)P_2$ which indicates a spin of $\frac{3}{2}$ and an admixture of $1\pm0.6\%$ quadrupole radiation with a phase angle of 0°.

VIII. RESONANCE WIDTHS

A. Direct Measurement

Over most of the energy region covered, the excitation curves were taken in steps of 2 kev. Practically all of the resonances rose from background to full height between successive points. On a few of the strongest resonances, data were taken at bombarding intervals of 50 ev with the result that the experimentally observed widths were equal to the energy spread of the beam, about 0.03% of E_p, or about $\frac{1}{2}$ kev. Since most of the targets were 2 kev thick or thicker, they all gave the "thick-target" resonance shape. The cross sections at resonance could not be determined from the data, so the yields were calculated in terms of $\int\sigma dE$, as discussed in Sec. III.

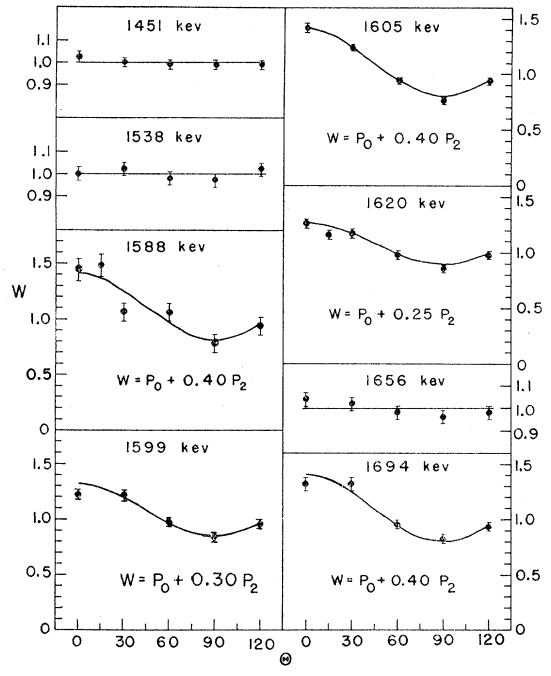

FIG. 16. The angular distributions of ground-state gamma rays from eight of the resonances in the $Ni^{60}(p,\gamma)Cu^{61}$ reaction. The curves were plotted from the illustrated equations. Note the displaced zero for the ordinate scale in the three isotropic distributions.

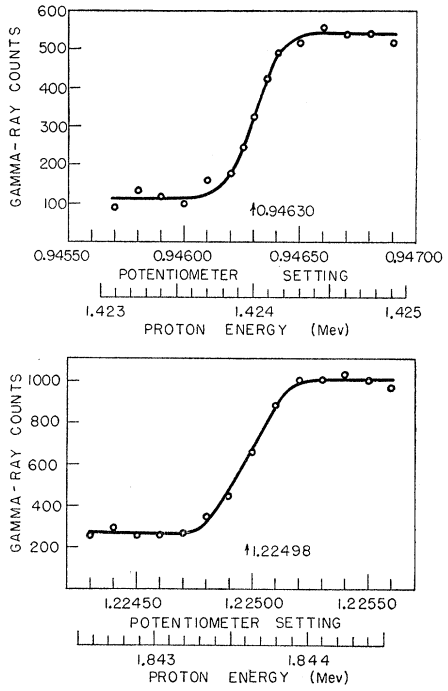

FIG. 17. The measurement of the precise bombarding energies at which two of the $Ni^{58}(p,\gamma)Cu^{59}$ resonances occurred, and their respective widths. A 2-meter-radius electrostatic analyzer was used. Absolute energy calibration uncertainty was $\pm0.05\%$, and beam inhomogeneity was between 0.016% and 0.022%.

Since the energy resolution of the NRL Nucleonics Division 2-Mv Van de Graaff accelerator was not adequate to measure the resonance widths, an attempt to measure the widths was kindly made by Dr. R. O. Bondelid using the NRL large Van de Graaff accelerator and its 2-meter-radius electrostatic analyzer.[4]

The results for the two most intense resonances in the Ni^{58} reaction, 1424 and 1844 kev, are shown in Fig. 17. For these data the gamma rays from a target about 4 kev thick to the incident protons, were detected with an unshielded 2-in.×2-in. NaI crystal and conventional electronics. The resonance yields do not rise as high above background as was observed in our excitation curves because of the higher background associated with the large Van de Graaff accelerator, the smaller amount of proton beam available from the high-resolution analyzer, and the use of an integral

discriminator instead of a differential type discriminator as was used for the excitation curves.

When the raw data shown in Fig. 17 are processed to remove the effects of beam inhomogeneity and Doppler broadening, upper limits can be given for the intrinsic resonance widths. These widths are 45 ev and 90 ev, respectively, for the 1424- and 1844-kev resonances. It should be emphasized that these are only upper limits; the widths could be essentially zero and still be consistent with the data.

B. Partial Gamma Widths

Even though the total widths of the resonances were so small that they could not be directly measured, values of one of the partial widths can be obtained from the cross-section measurements if it can be established which partial width is the smaller.

Since the first excited states of Ni^{58} and Ni^{60} are 1.45 and 1.33 Mev,[20] respectively, only two modes of decay are expected below these bombarding energies, namely radiative capture and elastic scattering. We ignore the possibility that a compound state C, formed by a proton of energy E_p, might decay by gamma-ray emission to a lower compound state C', where $E_\gamma<E_p$, with subsequent emission of a proton of energy E_p', where $E_p'=E_p-E_\gamma$.

Even for the maximum proton energy used, about 1.9 Mev, which is well above the threshold for conventional inelastic scattering, the transmission coefficient of the outgoing proton through the Coulomb barrier is so low that the partial width for such inelastic scattering is negligibly small. We shall therefore consider only the partial widths for radiative capture and elastic scattering.

The one-level Breit-Wigner formula for proton capture is usually written

$$\sigma=g\pi\lambda\!\!\!^{-2}\frac{\Gamma_p\Gamma_\gamma}{(E-E_r)^2+\frac{1}{4}(\Gamma_p+\Gamma_\gamma)^2}, \tag{2}$$

where g is a statistical factor, E_r is the proton energy at resonance, and Γ_p and Γ_γ are the proton and gamma partial widths, respectively. If we integrate $\sigma(E)$ with respect to E, we obtain

$$\int\sigma(E)dE=2g\pi^2\lambda\!\!\!^{-2}\frac{\Gamma_p\Gamma_\gamma}{\Gamma_p+\Gamma_\gamma}. \tag{3}$$

Now if we assume that $\Gamma_p\gg\Gamma_\gamma$, we get

$$\int\sigma dE=2g\pi^2\lambda\!\!\!^{-2}\Gamma_\gamma. \tag{4}$$

We now have a formula for determining Γ_γ from the experimental value of $\int\sigma dE$ for each resonance.

If instead we had assumed that $\Gamma_\gamma\gg\Gamma_p$ we would have obtained an identical formula for computation of Γ_p because the Breit-Wigner one-level formula for proton capture with no other competing reaction is symmetrical in Γ_p and Γ_γ.

For the partial gamma widths, it is useful to compare the observed values with Weisskopf's theoretical formulas,[23] which can be written, for the case of proton bombardment of nickel: $\Gamma_\gamma=1.67E_\gamma^3$ for $E1$ transitions, and $\Gamma_\gamma=0.021E_\gamma^3$ for $M1$ transitions.

Wilkinson[24] has compared the experimental partial gamma widths with the theoretical predictions of the Weisskopf formulas for about 100 cases involving very light nuclides ($A\leqslant20$) where the nature of the transitions was reasonably well established. He used the symbol $|M|^2$ to represent the ratio of experimental to theoretical width (or the experimental width in "Weisskopf units"). He found that "$E1$ transitions have a most probable speed of about 0.032 Weisskopf unit with a spread in speed of about a factor of seven either way," and that "the corresponding quantities for $M1$ transitions are a speed of 0.15 Weisskopf unit and a spread of a factor of 20 either way." He further noted "that if a transition shows a value of the quantity Γ_γ (ev) divided by E_γ^3 (Mev) of greater than 0.02, then there is a 10:1 chance that it is $E1$ rather than $M1$."

We can make use of Wilkinson's survey to test the validity of our assumption (in the cases where it is made) that $\Gamma_p>\Gamma_\gamma$, or to test the assumption of the parity of the resonant state, from which is determined the type of transition.

Kinsey[25] lists $|M|^2$ for about twenty dipole transitions resulting from thermal-neutron capture by medium and heavy elements. In order to obtain a fairly constant value of $|M|^2$, Kinsey found it necessary to make use of the correction factor D_0/D_B to the Weisskopf unit, where D_0 is the level spacing near the ground state, and D_B is the average spacing of levels near the radiating state of the proper spin and parity that they can combine with the given type of radiation to form the final state. This correction factor was given by Blatt and Weisskopf[26] to take into account configuration interaction, many-particle excitation, etc. For $E1$ radiation Kinsey found an average value of about 0.2 for $(D_0/D_B)|M|^2$, which he called $|M|^2$, for even-charge nuclides and about 0.01 for odd-charge nuclides, and ~0.1 for $M1$ transitions with no clear distinction between even- and odd-charge nuclides.

Wilkinson found (for $A\leqslant20$) no dependence of $|M|^2$ on A. This is not inconsistent with Kinsey's survey because (1) D_0/D_B for Wilkinson's nuclides is of the order unity, and (2) it is not clear how significant

[23] V. F. Weisskopf, Phys. Rev. 83, 1073 (1951).
[24] D. H. Wilkinson, Phil. Mag. 1, 127 (1956).
[25] B. B. Kinsey, *Beta- and Gamma-Ray Spectroscopy*, edited by K. Siegbahn (North Holland Publishing Company, Amsterdam, 1955), Chap. XXV.
[26] J. M. Blatt and V. F. Weisskopf, *Theoretical Nuclear Physics* (John Wiley and Sons, Inc., New York, 1952), Chap. XII.

configuration interaction, many-particle excitation, and allied effects are for Wilkinson's nuclides.

Since the average individual resonance intensity, $\int\sigma dE$, is approximately the same for Ni^{58}, Ni^{60}, and Co^{59} even though the relative level spacings were in the ratio of 10:2:1 over the energy interval 1.4–1.8 Mev, it is not clear that Γ_γ is dependent on the level spacing. As discussed below, it is possible that $\Gamma_p<\Gamma_\gamma$ in which case $\int\sigma dE$ would be proportional to the barrier transmission coefficients. For the present purposes, we shall consider $(D_0/D_x)|M|^2$ to be the significant quantity following Kinsey. We use D_x instead of D_B because our bombarding particles are not thermal, and the excitation energy of the compound state is therefore considerably in excess of the binding energy of the nucleon. Blatt and Weisskopf[26] used an estimate of about 0.5 Mev for the level spacing near the ground state, which is in agreement with the experimental observations in our case. In order to obtain a value of D_x, we shall assume that D_x equals twice the observed level spacing found from the excitation curves. Since the ground-state spins of Cu^{59} and Cu^{61} are both $\frac{3}{2}^-$, compound-state spins of $\frac{1}{2}$, $\frac{3}{2}$, and $\frac{5}{2}$ (resulting from s, p, d, and f-wave protons) can all emit dipole radiation to the ground state. If both parities are equally populated, half of the observed states could emit the same type of dipole radiation to the ground state.

C. Partial Proton Widths

The experimental intensity of each resonance was proportional to $\int\sigma dE$. If our assumption that $\Gamma_p\gg\Gamma_\gamma$ were true for all of the resonances observed, we would expect that the "envelope" of the resonances would follow Eq. (4), if we ignore individual resonance fluctuations. The only two quantities in Eq. (4) that depend on resonance energy are $\lambda\!\!\!^{-2}$ and Γ_γ. As the proton energy is increased, $\lambda\!\!\!^{-2}$ decreases, and Γ_γ varies in a somewhat complicated way depending on the branching ratios, multipolarities, and gamma-ray energies. If we consider only a dipole transition to the ground state, Γ_γ is proportional to E_γ^3, which means for the cases considered here that the change in Γ_γ almost exactly cancels out the $\lambda\!\!\!^{-2}$ change with proton energy. On the basis of these arguments we would therefore expect the resonance "envelope" to be relatively flat and constant. But as was discussed in Sec. VIIIB, Γ_γ is also affected by resonance density and is expected to decrease in proportion to the level spacing, D_x, which decreases rather rapidly with increasing proton energy as can be seen in Figs. 2, 3, and 4. So we would expect the resonance intensity, or $\int\sigma dE$, to drop with increasing density of levels. Or in other words, the average yield of quanta over a proton energy interval large enough to include a statistically satisfactory ensemble of resonances would be approximately constant as a function of proton energy.

That this is not the case can be seen immediately from Figs. 2–5. We note that the yield of quanta per unit proton energy exhibits an exponential type rise as a function of proton energy at least up to about 1.5 Mev. Figure 5, which illustrates the yield of quanta over the interval of the Co^{59} target (about 50 kev), shows the relevant quantities best.

On the basis of the above discussion, we conclude that somewhere below 1.5 Mev, our original assumption that $\Gamma_p\gg\Gamma_\gamma$ breaks down, at least for some of the resonances. Since all of the resonances below 1.3 Mev are relatively weak, it appears reasonable to assume for most of these resonances that $\Gamma_p<\Gamma_\gamma$. With this assumption, we are able to calculate Γ_p for these resonances, using Eq. (4) with Γ_p written in place of Γ_γ. Even if $\Gamma_p=\Gamma_\gamma$, our value of Γ_p would be incorrect by only a factor of two which is not disturbing since we are expecting only order-of-magnitude results.

We may compare these partial proton widths in a way analogous to that used above for the partial gamma widths, by removing the transmission factors, and comparing the resulting reduced widths, $\gamma_p^2=\Gamma_p/2T\rho$, with the Wigner single-particle limit, $\frac{3}{2}(\hbar^2/\mu R^2)$, using conventional symbols. Here we choose to define the reduced widths with dimensions of energy instead of energy times length as is sometimes done.

The barrier transmission coefficients could not be calculated for most of the proton energy range using the tables of Bloch *et al.*[27] because the ratio of proton energy to barrier height was lower than the region covered by their tables. The transmission coefficients were therefore calculated using the familiar WKB approximation method with an assumed contact radius of $1.45A^{\frac{1}{3}}\times10^{-13}$ cm. Since the arithmetic operations were considerable, a check on their accuracy was highly desirable. Such a check could be obtained using the curves of Morrison[28] provided one used the formulas $T_0=[(1-x)/x]^{\frac{1}{2}}e^{-2C_0}$ and $T_l=[(1+y-x)/x]^{\frac{1}{2}}e^{-2C_l}$, where x is obtained from his Fig. A-1 and y from his Fig. A-3. These formulas are different from those given by Morrison, but the symbols are the same as those used by Morrison except T is used here for his P.

The ratio of the reduced width to the single-particle Wigner limit is usually a more interesting quantity than the reduced width itself. The value of this ratio, a dimensionless quantity, designated by θ^2, is determined from the following formula derived from familiar relationships.

$$\theta^2=\frac{1.3\times10^{-8}\int\sigma dE}{g\lambda\!\!\!^{-2}T\rho}. \tag{5}$$

Here $\int\sigma dE$ is in units of ev-barns and $\lambda\!\!\!^{-2}$ is in units of

[27] Bloch, Hull, Broyles, Bouricius, Freeman, and Breit, Revs. Modern Phys. 23, 147 (1951).

[28] P. Morrison, *Experimental Nuclear Physics* (John Wiley and Sons, Inc., New York, 1953), first edition, Vol. II.

TABLE VII. For the resonances in the $Ni^{58}(p,\gamma)Cu^{59}$ reaction at proton energies E_p: the most reasonable value of incoming proton angular momentum l, the compound-state angular momentum J, the parity π, the partial gamma width Γ_γ, the partial gamma width for the ground-state transition $\Gamma_{\gamma 0}$, the corrected experimental matrix element for the ground-state transition $(D_0/D_x)|M|^2$ for the type radiation indicated, and lower limits of the dimensionless reduced proton width θ^2.

E_p (kev)	l	J	π	Γ_γ (ev)	$\Gamma_{\gamma 0}$ (ev)	$\frac{D_0}{D_x}\|M\|^2$	Type	θ^2 lower limit
1376	1	$\frac{3}{2}$	−	0.03	0.001	0.004	$M1$	4×10^{-4}
1424	1	$\frac{3}{2}$	−	0.3	0.1	0.2	$M1$	20×10^{-4}
1663	1	$\frac{1}{2}$	−	0.06	0.006	0.01	$M1$	1×10^{-4}
1716	1	$\frac{3}{2}$	−	0.07	0.04	0.1	$M1$	1×10^{-4}
1844	0	$\frac{1}{2}$	+	1	1	0.02	$E1$	2×10^{-4}

barns. A numerical check could be obtained by dividing the calculated reduced widths by Morrison's numerical estimate of the Wigner limit, his Eq. (73), p. 82, provided the right side of the equation were multiplied by 10, obtaining $\frac{3}{2}(\hbar^2/\mu R^2)\sim 30/A^{\frac{2}{3}}$ Mev.

D. Results

$Ni^{58}(p,\gamma)Cu^{59}$

For the Ni^{58} reaction, only two of the five angular distributions measured indicated isotropy, and one of these (the 1663-kev resonance) involved poor statistics. The other isotropic (with 1% statistics) distribution was that of the 1844-kev resonance. If we assume p-wave protons, that gamma transition is $M1$ and has a $(D_0/D_x)|M|^2$ value of 1.3 which is somewhat larger than any of the 10 examples of $M1$ neutron-capture radiation listed by Kinsey[25] but is well within the range of $|M|^2$ values listed by Wilkinson for $M1$ transitions for the very light nuclides. As will be brought out in Sec. IX, it is possible that we are observing a faster-than-average $M1$ transition. However, if we assume s-wave protons and therefore $E1$ radiation, the $(D_0/D_x)|M|^2$ value is 0.02 which means, if Wilkinson's criteria hold for the medium weight nuclides (after the factor D_0/D_x is applied), that there is a 10:1 chance that the radiation is $E1$. The essentially monoenergetic nature of the radiation further suggests $E1$ because of the relatively greater probability of $E1$ radiation than $M1$.[29] We therefore conclude that the evidence favors s-wave protons and even parity for the 1844-kev resonance.

TABLE VIII. For the resonances in the $Ni^{58}(p,\gamma)Cu^{59}$ reaction at proton energies E_p less than 1.3 Mev, where the assumption $\Gamma_p<\Gamma_\gamma$ is made: the values of the partial proton widths Γ_p, the reduced proton widths γ_p^2, and the dimensionless reduced widths θ^2. The reduced widths were obtained using s-wave penetrabilities.

E_p (kev)	Γ_p (ev)	γ_p^2 (kev)	θ^2
855	0.001	6	0.003
947	0.03	27	0.014
1010	0.002	0.6	0.0003
1100	0.01	1	0.0007
1227	0.01	0.4	0.0002

The 1663-kev resonance is best explained on the basis of $(D_0/D_x)|M|^2$ values if we assume p-wave protons, odd parity, and $M1$ radiation. The other three resonances all had angular distributions consistent with $J=\frac{3}{2}$, indicating either p-wave or d-wave protons. Since d-wave protons could also excite $J=\frac{5}{2}$ states, and since none of the angular distributions indicated a $J=\frac{5}{2}$ state, we conclude that p-wave protons were responsible. We therefore assign odd parity to the compound states and $M1$ as the type radiation. The $(D_0/D_x)|M|^2$ values are listed in Table VII. Also listed are lower limits of the dimensionless reduced widths calculated using the l value of protons indicated in the table. The $(D_0/D_x)|M|^2$ values for $M1$ radiation cover about the same range as the four examples listed by Kinsey for odd-charge nuclides.

As discussed above, it appears reasonable to assume that for all or most of the resonances below $E_p=1.3$ Mev, $\Gamma_p<\Gamma_\gamma$. On this basis, values of θ^2 have been calculated for these resonances using s-wave penetrabilities. If p waves and $J=\frac{3}{2}$ states are involved, θ^2 would be 50% too low. It is unlikely that d-wave resonances are observable for protons of such low energy. We therefore believe that Table VIII gives the correct order of magnitude for these θ^2 values. In any case, they are lower limits.

TABLE IX. For the resonances in the $Ni^{60}(p,\gamma)Cu^{61}$ reaction at proton energies E_p: the most reasonable value of incoming proton angular momentum l, the compound-state angular momentum J, parity π, the partial gamma width Γ_γ, the partial gamma width for the ground-state transition $\Gamma_{\gamma 0}$, the corrected experimental matrix element for the ground-state transition $(D_0/D_x)|M|^2$ for the type radiation indicated, and lower limits of the dimensionless reduced proton width θ^2.

E_p (kev)	l	J	π	Γ_γ (ev)	$\Gamma_{\gamma 0}$ (ev)	$\frac{D_0}{D_x}\|M\|^2$	Type	θ^2 lower limit
1451	0	$\frac{1}{2}$	+	0.3	0.3	0.02	$E1$	20×10^{-4}
1538	0	$\frac{1}{2}$	+	0.2	0.1	0.007	$E1$	6×10^{-4}
1588	1	$\frac{3}{2}$	−	0.2	0.05	0.2	$M1$	5×10^{-4}
1599	1	$\frac{3}{2}$	−	0.6	0.1	0.7	$M1$	13×10^{-4}
1605	1	$\frac{3}{2}$	−	0.5	0.4	1.7	$M1$	11×10^{-4}
1620	1	$\frac{3}{2}$	−	0.4	0.3	1.4	$M1$	9×10^{-4}
1656	0	$\frac{1}{2}$	+	0.5	0.4	0.02	$E1$	8×10^{-4}
1694	1	$\frac{3}{2}$	−	0.2	0.1	0.7	$M1$	3×10^{-4}

$Ni^{60}(p,\gamma)Cu^{61}$

For the Ni^{60} reaction, three angular distributions were isotropic resulting in $J=\frac{1}{2}$ assignments. Two of these (1451 and 1656 kev) have $(D_0/D_x)|M|^2$ values of 0.02 and are consequently assigned to type $E1$. The 1538-kev resonance has a lower $(D_0/D_x)|M|^2$ value,

[29] B. B. Kinsey and G. A. Bartholomew, Phys. Rev. 93, 1260 (1954).

0.007, but is also assigned as $E1$ because of the 70% branching ratio to the ground state. However, as will be seen later, $M1$ transitions sometimes showed high branching ratios to the ground state.

The other resonances all involve $J=\frac{3}{2}$ states and for reasons discussed above are assigned odd parity and $M1$ radiation. The $(D_0/D_x)|M|^2$ values are listed in Table IX as are also lower limits of θ^2. The $(D_0/D_x)|M|^2$ values for $E1$ radiation were inside the range covered by the eight examples listed by Kinsey for odd-charge nuclides. Some of the $(D_0/D_x)|M|^2$ values for $M1$ radiation were above the highest one of Kinsey's four examples, but were well within Wilkinson's distribution.

Table X lists the θ^2 values for the resonances under 1.3 Mev using the same assumption as discussed above for Ni^{58}.

IX. DISCUSSION

A. Experimental

Since nickel foils are commonly used as backings for solid targets and windows for gas targets, some of the more intense resonances can be used as secondary energy calibration points. Since natural nickel consists of 68% Ni^{58}, a thin natural nickel foil shows the Ni^{58} resonances very clearly. The two resonances at bombarding energies of 1424.1±0.7 and 1843.7±0.9 kev can be used as primary energy calibration points. Since their intrinsic widths are less than 45 and 90 ev, respectively, they can also be used to measure the inhomogeneity of a proton beam.

TABLE X. For the resonances in the $Ni^{60}(p,\gamma)Cu^{61}$ reaction at proton energies E_p less than 1.3 Mev, where the assumption $\Gamma_p<\Gamma_\gamma$ is made: the values of the partial proton widths Γ_p, the reduced proton widths γ_p^2, and the dimensionless reduced widths θ^2. The reduced widths were obtained using s-wave penetrabilities.

E_p (kev)	Γ_p (ev)	γ_p^2 (kev)	θ^2
725	0.002	40	0.02
895	0.002	4	0.002
1029	0.005	1	0.0006
1066	0.01	2	0.0008
1078	0.008	1	0.0005
1132	0.01	0.7	0.0003
1167	0.04	2	0.001
1197	0.04	1	0.0007
1209	0.04	1	0.0006
1239	0.04	1	0.0005
1247	0.03	0.7	0.0003

A second use of the resonances in a nickel foil backing or window is the determination of target thickness. For a solid target, the difference in bombarding energy between the appearance of a particular resonance on an uncoated foil, and on the target-coated foil gives the target thickness to the incident protons. Such a procedure could be used in determining stopping powers of various materials using weighed amounts of the material deposited on the foil. For gas targets, if nickel foils were used for both entrance and exit windows for the protons, the displacement of a resonance could be used to determine the thickness of the gas target, or its stopping power if the pressure were known. For both solid materials and a gas, the straggling of transmitted protons can be accurately determined by comparing both the width and yield of a resonance for direct protons and transmitted protons.

The ambient-cold-surface technique of protecting targets from vacuum system contaminants removes a severe restriction on certain types of experiments, the restriction being background from the same type reaction on carbon or fluorine. The fluorine problem has already been discussed. The $C^{12}(He^3,p\gamma)N^{14}$ reaction is fairly intense,[30] and the background from this reaction makes it very difficult to observe $(He^3,p\gamma)$ reactions on target nuclides with higher Z than carbon. Dr. R. O. Bondelid, using a 2-meter-radius electrostatic beam analyzer, has used the ambient-cold-surface technique to protect targets, such as Al, being used to make precise resonance energy determinations. With his equipment a relative shift in resonance energy of 25 to 50 ev would have been detectable during a ten-hour bombardment, but he observed no shift using a protected target.

Doppler broadening of a sharp threshold or narrow resonance because of the thermal motion of the target nuclei can also be somewhat reduced by cooling the target without simultaneously introducing the previously concomitant effect of building up contaminant films over the target, provided the target is protected in a manner similar to that described herein.

Since the 1844-kev resonance of Ni^{58} and the 1451-kev resonance of Ni^{60} involved essentially monoenergetic gamma rays of energies 5.23 and 6.24 Mev, they can be useful sources to test the response of spectrometers to gamma rays of these energies, and may be used as secondary energy calibration standards. The uncertainties in the gamma-ray energies as directly measured were ±0.02 and ±0.03 Mev, respectively. However, if one utilizes the isotopic reassignment of the neutron-capture gamma rays of Kinsey and Bartholomew[9] as discussed in Sec. IVB, and uses the Cu^{61} positron end point of Owen *et al.*,[12] the energy of the Ni^{60} proton-capture gamma ray can be calculated to be 6.24 Mev with an uncertainty of about ±0.01 Mev.

B. Theoretical

Previous to the present experiment, there were no known excited states of Cu^{59} or Cu^{61}. We are now aware of six bound states of Cu^{59} and 17 unbound or resonant states. In Cu^{61}, seven bound states were found and 54 resonant states. Shiffer *et al.*[31] performed a concurrent experiment observing inelastic scattering of

[30] Bromley, Almqvist, Gove, Litherland, Paul, and Ferguson, Phys. Rev. **105**, 957 (1957).
[31] Schiffer, Moore, and Class, Phys. Rev. **104**, 1661 (1956).

protons from Ni^{58} and found about 70 resonances at proton energies from 2 to 5 Mev.

The levels of the nuclei investigated in this experiment are of particular interest to the shell model. One aspect of possible interest is the apparent preference of negative parity for the more intense resonances. Most of the more intense resonances are probably $\frac{3}{2}^-$ states. This suggests the possibility that protons are captured in the $2p_{\frac{3}{2}}$ shell, which is the next shell above the just completely filled $1f_{7/2}$ proton shell of the nickel isotopes. The compound states are too high in energy and too narrow to be single-particle levels. A state having a reduced width equal to the full Wigner single-particle limit would have a laboratory width of one kev at a proton energy of about 1.5 Mev. But if the proton is captured in the $2p_{\frac{3}{2}}$ shell, while at the same time raising one or two pairs of nucleons from the $1f_{7/2}$ shell (occupied by both protons and neutrons) or the $2p_{\frac{3}{2}}$ shell (occupied in nickel by neutrons only) to higher shells, perhaps the $1f_{\frac{5}{2}}$ or $2p_{\frac{1}{2}}$ shells, both the high excitation energy and relatively small widths could be accounted for, at least qualitatively.

Nussbaum[32] lists experimental values for single-particle level spacing in the region of the $1f_{7/2}$ shell. He gives the $2p_{\frac{1}{2}}-2p_{\frac{3}{2}}$ spacing to be $\sim$2 Mev, and the $1f_{\frac{5}{2}}-1f_{7/2}$ spacing to be $\sim$1.3 Mev. If we assume that these spacings would not change greatly even if several nucleons were raised to higher shells, one or two pairs of nucleons raised from the $1f_{7/2}$ shell or the $2p_{\frac{3}{2}}$ shell to one of the higher shells could account for all of the energy of excitation of the compound states. If one or two pairs of nucleons were so raised, and if their spins and angular momenta added vectorially to zero, the net spin of the compound state would be just that of the proton captured in the $2p_{\frac{3}{2}}$ shell, that is, $\frac{3}{2}^-$.

In spite of the evidence indicating that the 1844-kev resonance of Ni^{58} is excited by s-wave protons and emits $E1$ radiation, it could conceivably involve proton capture in the $2p_{\frac{1}{2}}$ shell with the raising of perhaps the pair of neutrons in the $2p_{\frac{3}{2}}$ shell to the $2p_{\frac{1}{2}}$ shell. The resulting $M1$ transition to the ground state could then be considerably faster than average in accord with the observations. The essentially 100% ground-state transition from this compound state clearly suggests a great deal of similarity in the configurations of the two states. We therefore feel that some justification exists for postulating the rather simple mechanism described above.

A further suggestion coming from the ground-state preference for transitions from the 1844-kev resonance and others is that the doubly-closed core of 28 protons and 28 neutrons remains relatively intact. We would not expect, for example, a strong gamma-ray transition which involved changing a nucleon from an f shell to a p shell or vice versa. The fact that no ground-state transitions were observed during the bombardment of Co^{59} supports this view. One would expect that the ground-state transition would be somewhat inhibited on the basis of selection rules alone, but one would still expect to observe some ground-state transitions. An upper limit of about 0.1% could be placed on the branching ratio to the ground state. The same reasoning can be applied to the branching ratio to the 1.33-Mev state. On the basis of selection rules alone, this transition should not be inhibited because dipole radiation and quadrupole radiation are both possible for protons with every l value from 0 to 6. The energy dependence of partial gamma-ray widths also favors transitions to the 1.33-Mev state over higher states, but less than 5% of the transitions were to the 1.33-Mev state. We therefore conclude that with proton bombardment of the nickel isotopes, we are indeed observing shell model phenomena, and that the core itself remains relatively undisturbed (that is, if a $1f_{7/2}$ nucleon is disturbed, it is only to the extent of flipping its spin in going to the $1f_{\frac{5}{2}}$ shell).

The resonance density for the Ni^{60} reaction was about five times as great as for the Ni^{58} reaction for proton energies of 1.4–1.8 Mev. Only a small part of this difference in density of states can be accounted for by the different excitation energies resulting from the different Q values. From the well-known theoretical prediction that the density of states is proportional to $\exp(aE^{\frac{1}{2}})$, we would expect the density of states to increase by only about 30% in going from the excitation energy in Cu^{59}, $\sim$5.0 Mev, to the excitation energy in Cu^{61}, $\sim$6.4 Mev. It seems more likely that the larger density of states for the Ni^{60} case stems from the larger number of configurations available to the larger number of nucleons outside the doubly-closed core of 28 protons and 28 neutrons. A similar argument could be made concerning the very high level density in the Co^{59} reaction. This point lends further credence to the idea that in the nickel reactions we are observing for the most part excitation of the nucleons outside the core, leaving the core itself relatively intact, in spite of the absence of general evidence for a strong shell closure at nucleon number 28.

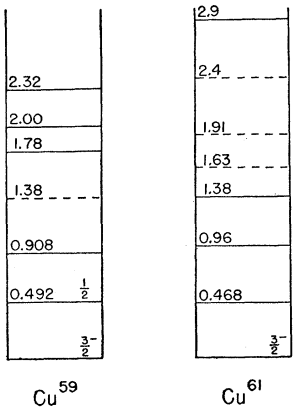

FIG. 18. The low-lying energy levels of Cu^{59} and Cu^{61}.

[32] R. H. Nussbaum, Revs. Modern Phys. 28, 423 (1956).

The similarity of the low-lying level structures of Cu^{59} and Cu^{61} as illustrated in Fig. 18 is rather striking. It is not clear why this similarity exists, because one might expect a closer low-lying level spacing in Cu^{61} than in Cu^{59} as is observed in the resonance density. The level structures of these two copper isotopes will be compared with the nickel isotopes of the same mass numbers in a forthcoming publication.[33]

[33] J. W. Butler and C. R. Gossett (to be published).

X. ACKNOWLEDGMENTS

The authors wish to acknowledge the aid of Dr. H. D. Holmgren in the taking of the data for the excitation curves, and to Mr. Glen Stassen for helping take the data for the angular distributions, and wish to thank Dr. R. O. Bondelid for making the precise energy determinations of two of the resonances, and for determining a low upper limit to the width of the same two resonances.

PHYSICAL REVIEW VOLUME 108, NUMBER 6 DECEMBER 15, 1957

Decay of Ca^{38}†

J. E. Cline and P. R. Chagnon
Physics Department, University of Michigan, Ann Arbor, Michigan
(Received August 2, 1957)

The decay of a new isotope, Ca^{38}, produced by the reaction $Ca^{40}(\gamma,2n)$, has been observed via branching of the beta decay to a 3.5-Mev excited state of K^{38}. The observed half-life of (0.66±0.05) second is consistent with a log (*ft*) value of 3.5 for the ground-state transition. The tentative assignment for the K^{38} excited state is $J=1^+$, $T=0$ although $J=0^+$, $T=1$ is also possible. A search for branching in the decay of S^{30} is also discussed.

INTRODUCTION

INTEREST in the odd-odd, self-conjugate ($N=Z$) nuclei has led to a search for their parent ($N=Z-2$) isobars and the modes of decay of the latter. Moszkowski and Peaslee[1] have pointed out that several of these $N=Z-2$ isobars may be produced by photonuclear reactions on stable targets, and have suggested that branching of their beta decays should usually occur. The $N=Z-2$ ground state (0^+, $T=1$) in general decays by superallowed positron emission to the corresponding isobaric-triplet level of the self-conjugate nucleus; if a (1^+, $T=0$) excited level of the latter lies energetically below the ground state of the $N=Z-2$ nucleus, then branching should take place by allowed positron decay to this state, with subsequent $M1$ gamma-ray emission.

Kofoed-Hansen[2] has pointed out that for the superallowed transitions, the log(*ft*) value should be 3.5 in all cases. The disintegration energy may be calculated from nuclear-mass systematics, and from this and the *ft*-value, the half-life may be predicted. In particular, for the ground-state decay of Ca^{38}, Kofoed-Hansen predicts a positron end-point energy of 5.21 Mev and a half-life of 0.7 sec. The observed lifetime would, of course, be somewhat shorter if branching occurs.

EXPERIMENTAL CONSIDERATIONS

Thick targets (≈10 g/cm²) of Ca and CaH_2 have been exposed to the 85-Mev bremsstrahlung beam of the Michigan electron synchrotron. The targets were viewed by a NaI(Tl) scintillation spectrometer and single-channel pulse-height analyzer, signals from which were then analyzed in time with a 20-channel time-delay analyzer. An electronic timing circuit, synchronized to the accelerator cycle, was used to operate alternately the accelerator and the analyzing equipment. Thus annihilation radiation from the positron decays, or nuclear gamma rays, could be selected by the single-channel analyzer and their decays analyzed with the 20-channel delay analyzer. In most cases the decays were followed for several half-lives; the half-lives quoted are taken from least-squares fits to these data.

When Ca^{40} is irradiated with high-energy x-rays, the predominant reactions, in order of intensity, are $Ca^{40}(\gamma,n)Ca^{39}$ and $Ca^{40}(\gamma,np$ or $d)K^{38}$. Ca^{39}, K^{38}, and K^{38m} are all positron emitters; both Ca^{39} and K^{38m} have lifetimes of the order of 0.9 sec and both have end points of the order of 5 Mev. Hence it would be exceedingly difficult to identify the ground-state transition from Ca^{38}, produced by the weaker reaction

TABLE I. Delayed gamma radiation observed after irradiation of potassium and calcium targets. The term mc^2 indicates two-quantum annihilation radiation.

Target	Gamma-ray energy	Observed half-life	Assignment
K^{39}	mc^2	7.67±0.03 min	$K^{38}(\beta^+)A^{38*}$
K^{39}	2.18 Mev	7.67 min	$A^{38*}(\gamma)A^{38}$ after $K^{38}(\beta^+)A^{38*}$
K^{39}	mc^2	0.951±0.007 sec	$K^{38m}(\beta^+)A^{38}$
Ca^{40}	mc^2	0.89 sec	$Ca^{39}(\beta^+)K^{39}$ *and* $K^{38m}(\beta^+)A^{38}$
Ca^{40}	mc^2	7.67 min	$K^{38}(\beta^+)A^{38*}$
Ca^{40}	2.18 Mev	7.67 min	$A^{38*}(\gamma)A^{38}$ after $K^{38}(\beta^+)A^{38*}$
Ca^{40}	3.5±0.1 Mev	0.66±0.05 sec	$K^{38*}(\gamma)K^{38}$ after $Ca^{38}(\beta^+)K^{38*}$

† Work supported by a contract with the U. S. Atomic Energy Commission.
[1] S. A. Moszkowski and D. C. Peaslee, Phys. Rev. **93**, 455 (1954).
[2] O. Kofoed-Hansen, Phys. Rev. **92**, 1075 (1953).